DISSERTATION FOR THE DEGREE OF DOCTOR OF PHILOSOPHY (PHD)

Development of personal nasal protective device and device for formulated nanoparticles

by Thinh To Quoc PharmD

UNIVERSITY OF DEBRECEN
DOCTORAL SCHOOL OF PHARMACEUTICAL SCIENCES

DEBRECEN, 2025

DISSERTATION FOR THE DEGREE OF DOCTOR OF PHILOSOPHY (PHD)

Development of personal nasal protective device and device for formulated nanoparticles

by Thinh To Quoc PharmD

Supervisor: Zoltán Ujhelyi PharmD Habil. PhD

UNIVERSITY OF DEBRECEN
DOCTORAL SCHOOL OF PHARMACEUTICAL SCIENCES

DEBRECEN, 2025

TABLE OF CONTENTS

1. INTRODUCTION 7
1.1. The role of nasal drug therapy in modern drug therapies 7
1.2. The role of personal nasal protective device therapy in respiratory pandemics 9
1.3. The importance of Individual Nasal Filters in Modern Air Quality Management 11
1.4. Nasal Filter Design and Development: Harnessing Technology for Respiratory Health 12
1.5. The Operational Principles of Healthcare Nasal Filters: Design Perspectives 13
2. OBJECTIVES 14
3. DESIGN AND PROTOTYPE DEVELOPMENT OF A CUSTOM NASAL FILTERS 15
3.1. Design of the Nasal Internal Filter MK.1 (Mark 1) 16
3.2. Design of the Nasal Internal Filter MK.2 (Mark 2) 19
3.3. Design of the Nasal Internal Filter MK.3 (Mark 3) 21
3.4. Design of the Nasal Internal Filter MK.4 (Mark 4) 22
3.5. Design of the Nasal Internal Filter MK.5 (Mark 5) 22
4. ASSESSMENTS AND PERFORMANCE TESTS 28
5. FDM TECHNOLOGY, 3D PRINTING, AND ITS COMPONENTS 36
5.1. Foundations of instrument development 36
5.2.Applied Filaments for FDM printing 37
5.2.1.MD1 FLEX 37
5.2.2. PLA 37
5.2.3. TPU 38
5.3. Applied Software for design 40
6. NEF DESIGN AND PROTOTYLE PRODUCTION 42
6.1. Applied filter for NEF 43
6.2. Incorporation of the filter into NIF 44
6.3. Shape fit tests and results 45
6.4. Design and prototype production of Powder Inhaler 47
7. INTEGRATION OF NASAL FILTERS WITH DRUG DELIVERY SYSTEMS 48
7.1. Solid nanoparticles for nasal formulations 48
7.2. Materials 51
7.3. Formulation of compositions 52
7.4. Formulation of Solid Nano Carriers 52
7.5. Scanning Electron Microscopy 53

7.6. Determination of Droplet Size 53
7.7. Evaluation of particle disintegration 53
7.8. Evaluation of active ingredient dissolution 53
7.9. Stability tests 53
7.10. CPZ Content Determination 54
7.11. Cell Culturing 55
7.12. MTT Viability Assay 55
7.13. Animals and sample collection 55
7.14. Sample preparation for animal experiments 56
7.15. Gas chromatograph-mass spectrometric (GC-MS) analysis 56
7.16. Statistical Analysis 57
8. RESULTS 58
8.1. Selection of core materials and excipients for nasal particles 58
8.2. Setting formulation parameters 60
8.3. Determination of particle size and distribution 61
8.4. Evaluation of size and morphology of solid nanostructures 63
8.5. Evaluation of the possible cytotoxic effect 65
8.6. CPZ dissolution measurements 66
8.7. Animal studies of CPZ utilization 68
9. DISCUSSION 70
10. SUMMARY 73
11. REFERENCES 74
12. LIST OF PUBLICATIONS THE DISSERTATION IS BASED ON 89
13. KEYWORDS 90
14. LIST OF ABBREVIATIONS 91
15. ACKNOWLEDGMENT 95
16. FUNDING 96

ABSTRACT

Nasal drug intake has been a priority in scientific research for decades, as it offers many advantages in the targeted delivery of active ingredients. Various drug delivery systems and devices are being developed, which significantly contribute to increasing the effectiveness of therapies and patient comfort. The advantages of intranasal drug administration are indisputable, since the nasal mucosa provides an excellent surface for quick and effective absorption of active ingredients. The large expansion of the nasal surface and intensive absorption allow certain active substances to enter directly into the central nervous system bypassing the blood-brain barrier. Pharmaceutical forms that can be administered to the nose are typically solutions or liquid-dispersed systems such as emulsions and suspensions. In recent years, the development of nanostructured drug carriers has undergone significant development. Solid phase heterogeneous disperse systems represent a new direction in pharmaceutical technology, allowing the effective delivery of a wide range of active ingredients. The aim of our research was to create a solid drug delivery system that combines the known benefits. In the application of nanoparticles, we not only exploited the size advantages, but also used the adhesion and penetration enhancing properties of the excipients to increase efficiency. In addition to medicated nasal treatments, nowadays more and more emphasis is placed on respiratory protection, both infectious and non-infectious, but against harmful environmental influences. In addition to diseases caused by environmental pollution, more and more attention is being paid to the possibilities of personalized protection against various pathogens. In the development of innovative protective equipment, not only medicine, but also engineering and technological research play a prominent role. One promising solution is to use customized nasal filters that provide effective protection against environmental pollutants and pathogens. These tiny nasal devices can individually filter out dirt, allergens and microorganisms from the air we breathe. Another benefit of personalized nasal filters may be that they can help boost your immune system. These devices offer medicine the opportunity to adapt protection to the genetic and immunological peculiarities of the individual. During development, the goal is not only to increase the efficiency of the devices, but also to take into account user needs, since convenience and portability are key factors in successful application. Industrial research is increasingly striving to translate technological innovations into easy-to-use forms in everyday life. Based on this, it can be concluded that customized nasal filters offer an innovative and promising opportunity to protect against air pollution and pathogens. Through technological research and development, these

devices can have a significant long-term impact on both human health and the environment. New, unique solutions and ongoing research give us hope that in the future we will be able to protect our health in even more effective and sophisticated ways, despite ever-changing environmental challenges.

1. INTRODUCTION

1.1. The role of nasal drug therapy in modern drug therapies

The use of drugs that can be injected into the nose has long been in the center of scientific interest, since the beneficial properties of the nasal mucosa promote the absorption of active ingredients. The nose lining not only offers a big area for taking in active parts, but it also helps the medicine get straight to the brain, skipping the blood-brain barrier [1]. Also, breaking down drugs in the liver may be lessened, boosting how well they work [2]. Many studies have shown that different active things, including big bits like proteins and peptides can be taken in through the nose into general flow especially when helpers that make things easier to pass are used. The importance and availability of nasal drugs of systemic action is constantly increasing [3]. The use of these preparations is especially beneficial for diseases that require quick and effective treatment. Nasal pharmaceutical forms are mostly solutions or liquid-dispersed systems such as emulsions and suspensions [4]. Although these dosage forms are easy to prepare and their stability is excellent, patients often complain that fluid flows down the pharynx, resulting in an unpleasant taste [5]. From a pharmacological point of view, another challenge is the rapid elimination of active substances. Such problems can be corrected by using appropriate excipients that increase adhesion and prolong drug retention [6]. The aim of the research was to produce and investigate new solid lipid nanoparticles to increase the penetration of the active substance. In addition to the API formulation, an innovative nasal medicine delivery device was developed, which was later tested. Chlorpromazine (CPZ), which is an antagonist of dopamine receptor D2 and receptors D3 and D5, is primarily used to treat psychotic disorders such as schizophrenia and bipolar disorder [7]. In this research, chlorpromazine was chosen as the active ingredient because it is analytically well characterized and reducing its therapeutic dose can reduce common and serious side effects. These include dyskinesia, drowsiness, dry mouth, orthostatic hypotension, and weight gain [8]. Serious adverse reactions include tardive dyskinesia, neuroleptic malignant syndrome, seizure threshold reduction and leukopenia. It may increase the risk of death in elderly dementia patients and its safety during pregnancy is unclear [9]. Nanoparticles, as modern therapeutic systems, have ushered in a new era in drug administration. These systems allow targeted delivery of the active substance to tissues and cells while minimizing systemic side effects and toxicity [10]. As a result, new

opportunities have opened up in the diagnosis and treatment of various diseases. Due to the wide range of applications of nanoparticles, they can play an important role in the treatment of serious diseases such as tumors [11]. Biodegradable nanoparticles can be produced, for example, using polylactic acid (PLA), polylactic glycolic acid (PLGA) or polymethyl methacrylate (PMMA) [12]. Polymer-drug conjugation allows targeted therapy, which is especially effective when penetrating amphiphilic excipients are used. Surfactants are widely used in pharmaceutical technology developments, especially to improve the bioavailability of water-insoluble drugs [13]. These substances are able to modify the structure of permeability barriers, promoting better absorption of active substances. However, they can also cause local irritation and cell damage as disadvantages, therefore in vitro cytotoxicity studies are essential [14]. Studies have shown that the combination of penetrating substances and polymers is a promising option for increasing the efficacy of active substances [15]. Self-assembling emulsion systems can be formed by titrimetric dilution with appropriate surfactant combinations. Since safety is of paramount importance for all medicinal products, the developed systems have been subjected to biocompatibility tests. The applied tests were performed on RPMI 2650 immortalized nasal epithelial cell lines with MTT viability test, which confirmed biocompatibility [16]. Currently, one of the most dynamically developing areas of pharmaceutical technology is the production of nanoscale carrier systems [17]. During our experiments, the formulation technique was selected based on reliability and efficiency. Spray drying technology, which has shown outstanding development in recent years, is one of the most promising methods [18]. The solid-phase nanoparticles were produced with the Büchi Nano Spray Dryer B-90 HP, which is ideally suited for laboratory nanoparticle formulations. The production of nanostructures takes place in four steps: sample preparation, atomization and drying of droplets, capture of particles on the electrode, and recovery of the final powder [19].

The physical parameters of the nanoparticles were analyzed with Malvern Nano Zetasizer ZSP [20], while morphological analysis was performed by scanning electron microscopy (SEM) [21]. The accurate and efficient administration of nano powders also required the development of a unique dosing device, which was made with FDM 3D printing technology. The devices were designed taking anatomical features into account, and then fine-tuned based on feedback from volunteers. Our results may provide useful data for future developments in nasal drug delivery systems.

1.2. The role of personal nasal protective device therapy in respiratory pandemics

Recent epidemiological events have brought about significant changes in people's behaviour and attitudes towards personal protection [22]. Mask-wearing, hand hygiene, social distancing, telecommuting and vaccinations have become integral parts of our everyday lives during the protection against the virus [23]. These behavioural changes have reinforced the recognition that individual and collective responsibility is key to the effective management of infectious diseases [24]. While some protective measures may reduce the further spread of the pandemic, others may have long-term impacts on social norms and practices [25]. In the post-pandemic era, the lessons learned through behavioural change are likely to contribute to addressing future pandemics and other public health crises [26]. Continued advancement of public health knowledge, easy access to health care and effective communication between governments and communities will be essential to maintain protective behaviour in the coming decades [27]. Respiratory diseases may pose a more serious threat to other infections, considering how the infection spreads, the importance of the respiratory system, and the potential for rapid spread in communities [28]. Such diseases pose significant health risks because they are spread through respiratory droplets, usually in the form of viruses or bacteria that can be inhaled by other people [30]. This type of spread makes them particularly contagious, especially in crowded, confined spaces. Respiratory infections are accompanied by various symptoms [31], which can range from breathing discomfort to severe difficulties that can greatly reduce quality of life [32]. Some infections can worsen quickly, leading to acute respiratory distress syndrome (ARDS), which can cause severe pneumonia and may require mechanical ventilation. In ARDS, damage to the lungs compromises oxygen exchange. COVID-19, SARS, and MERS can also cause severe respiratory illnesses [33], often associated with extremely high mortality, especially among the elderly, children, and chronically ill. Other respiratory diseases, such as flu and cold viruses, cause seasonal outbreaks [34], which can put a heavy strain on healthcare systems, especially during epidemics. Although some respiratory infections can be treated with antiviral medications, treatment options for other viruses are limited. Vaccines against them already exist, but vaccines against seasonal or new agents with genetic mutations can take a long time to develop. Influenza and coronaviruses, such as RNA viruses, are capable of rapid mutation [35], which can lead to the emergence of new, higher virulence strains, thus complicating vaccine development. In addition to infectious agents, it is important to take into account the effects of increasing air pollution, which also aggravate the

situation. Air pollution reduction has been at the heart of health problems for decades [36], but it has now become a global problem affecting millions of people worldwide. The health effects of air pollution are already widely known, and research has confirmed its long-term adverse effects [37]. Air pollution increases respiratory diseases such as chronic obstructive pulmonary disease (COPD), asthma, and acute respiratory infections [38]. Due to the different particle sizes of harmful substances, protection is particularly difficult (Figure 1). Many substances are particularly dangerous because they can penetrate deeper areas of the lungs and cause inflammation in the bloodstream [39]. Several studies have shown that air pollution increases the risk of cardiovascular diseases such as heart attack, stroke, and hypertension [40]. In addition to long-term air pollution, it increases the risk of lung cancer and other cancers, including bladder and breast cancer [41]. Substances in polluted air can also cause neurological disorders such as Alzheimer's and Parkinson's disease [42]. Research has shown that prenatal air pollution is associated with adverse birth outcomes such as low birth weight, premature birth, and developmental problems [42]. The adverse effects resulting from air pollution clearly show that air purification is of paramount importance not only from a health point of view, but also from an epidemiological point of view [43].

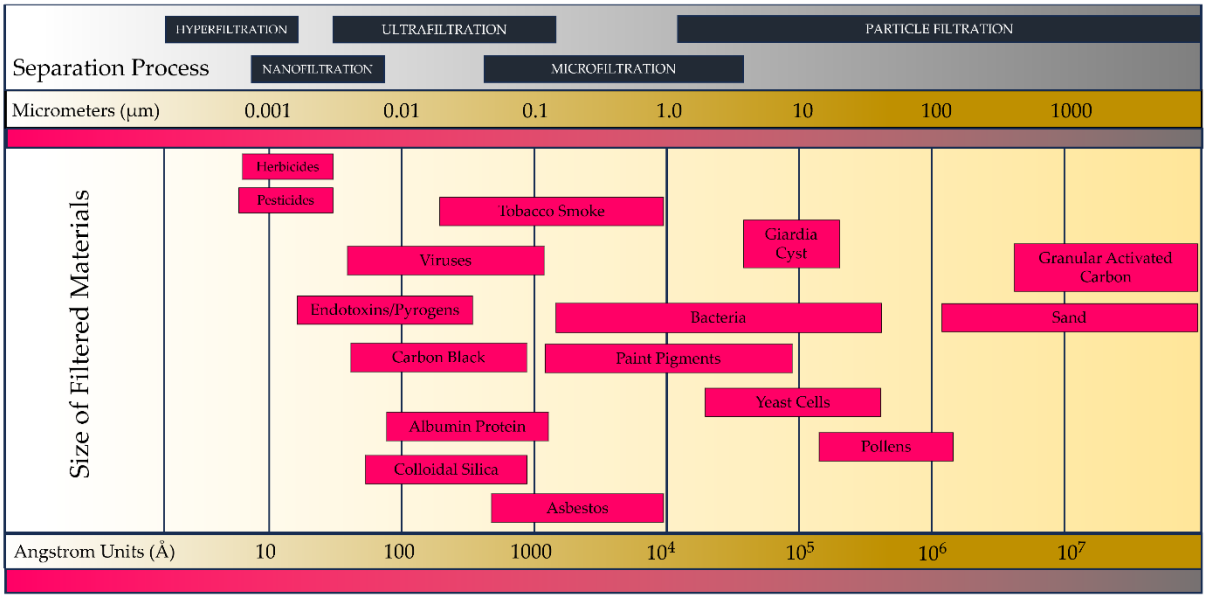

Figure 1. Sizes of filtered materials (µm and Å) and possible separation processes.

1.3. The importance of Individual Nasal Filters in Modern Air Quality Management

Modern air quality management (AQM) systems are based on complex, strategic solutions. Various tools can be integrated into the sorter (Figure 2). Nasal filters are usually small, devices that, when discreetly placed in the nostrils, act as a mechanical barrier to prevent particles and pollutants from entering the airways [44]. They are usually made of hypoallergenic materials [45]. One of the biggest advantages of nasal filters is their ability to protect our respiratory system from various pollutants in the air [46]. As a result, they provide protection against respiratory irritants, reducing the risk of developing allergies, sinus infections, and other respiratory problems [47]. By preventing harmful particles from entering the lungs, nasal filters can play a significant role in protecting the respiratory system [48]. The biggest advantage of these tools is that they provide solutions to multiple problems individually [49]. Nasal filters are a practical and convenient solution for maintaining clean air. Their compact size and ease of use make them a portable and discreet option for people of all ages. Unlike masks or respirators, nasal filters do not obstruct the face, making it more comfortable to wear for extended periods of time [50]. Plus, they are disposable or easy to wash, ensuring regular replacement for optimal operation. In the broader context of air quality management, the use of nasal filters can bring environmental benefits. By providing personalized clean air, these filters can reduce the need for energy-intensive air purifiers and contribute to reducing your carbon footprint [51].

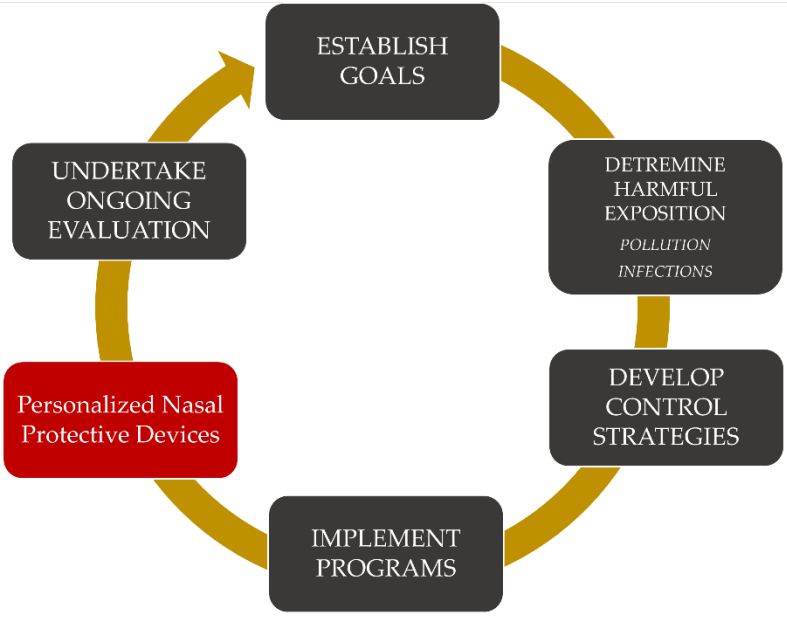

Figure 2. Implementation of personal nasal filters in AQM systems.

1.4. Nasal Filter Design and Development: Harnessing Technology for Respiratory Health

The aim of developments nowadays is to develop effective and personalized nasal filters using the latest technologies [38]. Materials science plays an unquestionably key role in the development of nose filters. Research involves testing new, biocompatible, hypoallergenic materials [42]. The development of nanotechnology has made it possible to produce nanofiber filters that provide excellent filtration performance without compromising breathability. Due to their sophistication, these filters can effectively block fine particles, allergens, and even harmful microorganisms [52]. Computational fluid dynamics modeling (CFD) has established and now serves as a proven tool in simulating and investigating nasal airflow dynamics [53]. CFD simulations can effectively help fine-tune filter geometry and size, reducing the chance of air leakage at the edges of the filter [54]. Three-dimensional printing and rapid prototyping offer new possibilities for fast and cost-effective design of nose filters [55]. Thanks to these technologies, it is now possible for researchers to receive real-time feedback from users while experimenting, allowing them to refine designs before mass production [56]. In addition, it is important to emphasize that the development of sensor technology has opened up new horizons for intelligent nose filters [48]. Filters integrated into sensors can monitor air quality in real time and provide information on both the presence of pollutants and health risks [49].

This improved technology ensures that plastic waste and pollution is not growing simultaneously with the process [46]. Moreover sustainable, biodegradable filters might offer a green alternative. Chitosan, a well known biodegradable polymer, has great potential in developing nasal filters due to its ability to adhere to the nasal mucosa and provide long-term release of active ingredients [58]. Biodegradable polymers such as polylactic acid (PLA) and poly(l-lactic acid-co-glycolic acid) (PLGA) are promising in drug administration and are able to encapsulate drug molecules, protecting them from degradation and providing directional release [59]. Biodegradable hydrogels can also be used as drug carriers, providing a slow release of drugs while providing a biocompatible environment for drug transport and absorption.

1.5. The Operational Principles of Healthcare Nasal Filters: Design Perspectives

A key factor in the usability of health nose filters, in addition to effectiveness, is shape and fit. A well-designed filter should adapt to the structure of the nasal passages, providing thorough coverage and secure sealing. Proper airflow control is, of course, vital to nose filter performance [55]. The filter must strike a balance between easy breathing and sufficient airflow, while providing sufficient resistance to trapping harmful particles [50]. Health nose filters rely on both mechanical and electrostatic filtration processes. The design of the material used to create them ensures an optimal combination of surface filling and filtration efficiency. Among users, convenience and efficacy play the most important role in applying [50]. To enhance compliance, filters are designed to be lightweight, non-intrusive, and gentle on the nasal passages. In addition, hypoallergenic materials also help minimize the risk of irritation or allergic reactions, allowing their use by a wider range of individuals. Durability and reusability are also key considerations when designing health nose filters. By using durable materials and modular design, manufacturers can create filters that can withstand repeated use and cleaning [51]. The design principles behind health nose filters focus not only on performance, but also on optimizing comfort and user experience. By carefully considering factors such as shape, fit, airflow, filtration, comfort, stability and durability, designers create filters that provide effective protection against airborne pollutants and allergens. These design strategies evolve as materials and technology evolve, positioning health nose filters as vital tools for maintaining respiratory health in a variety of environments

2. OBJECTIVES

Our research and development activities aimed to create an innovative nasal protective device and a specialized drug delivery system that combined the benefits of nasal filtration and drug administration. The main objectives were the following:

We aimed to create a nasal filter with market potential, capable of providing effective protection against inhaled harmful substances and pathogens.

Our goal was to create a device that could be used both for air filtration and the intranasal administration of pharmaceutical compounds.

To enhance intranasal drug delivery, our aim was to develop different nanometer-sized drug carrier systems composed of penetration-enhancing excipients. These systems optimized the efficiency of drug absorption through the nasal mucosa.

A key goal was to conduct detailed analyses of the physical and chemical properties of the drug delivery systems. Additionally, our aim was to emphasize safe application by subjecting the nanocarrier systems and their components to rigorous biocompatibility tests.

Our aim was to establish a solid scientific foundation that could contribute to the long-term advancement of intranasal drug formulation and the development of personalized protective devices in the pharmaceutical industry and healthcare innovation.

3. DESIGN AND PROTOTYPE DEVELOPMENT OF A CUSTOM NASAL FILTERS

Respiratory allergies and diseases are commonly caused by airborne allergens present in our environment. While improving overall air quality is an arduous and often impractical task, current efforts to mitigate air pollution frequently exacerbate the problem rather than solve it. Given these limitations, enhancing personal protective equipment (PPE) represents a more feasible and immediate solution. An ideal PPE should be simple, cost-effective, efficient, durable, and aesthetically unobtrusive. At present, surgical masks are the most commonly used form of airway protection. Despite significant advancements since their inception centuries ago, masks alone do not provide adequate protection against all airborne hazards. On the other hand, gas masks, while highly effective, are impractical for daily use due to their bulky design. The situation detailed above inspired the project, in which we apply a new approach to creating a unique nasal filter. The nasal filtration system consists of two subtypes: the nasal internal filter (NIF) and the nasal emergency/ external filter (NEF). These small portable individual devices are discreet, allowing users to wear them without any hassle wearing them. In operation, the device uses exclusively physical mechanisms, does not require external support, for example, a power source. It offers a wide range of customizable options to meet individual needs and ergonomic protection specifically for the nasal passages, which serve as the primary interface for air exchange between the body and the external environment. The improved nose filter can be considered a miniature, highly effective gas mask, designed to fit perfectly into the nasal cavity, providing targeted protection against airborne contaminants while maintaining user comfort and convenience, which was the most important goal of the project.

3.1. Design of the Nasal Internal Filter MK.1 (Mark 1)

The first prototype, designated is the MK.1. This device comprises two main components: the Shell and the Mobile Phase. The Static Phase called the Shell serves as the structural framework, encapsulating the entire mechanism and providing the interface with the user's nasal cavity. Located directly behind the nostril, Shell is designed in a circular or ergonomic shape to provide an optimal fit and comfort for each user. The inner wall of Shell is made of polymer so robust and durable that it guarantees precise and reliable mobility of internal components. In contrast, the outer layer is coated with a soft, flexible polymer to match the individual contours of each user's nasal cavity, increasing comfort and stability. In the design, it is clear that the mobile phase includes the tunnel, which performs two main functions. First of all, it acts as a housing for the filter core, which is considered a critical element of the filtration mechanism. Secondly, it can be seen that the tunnel plays a central role in the bidirectional airflow system, which is a unique feature of the nose filter, which we developed within the framework of the Project Divine Wind initiative.

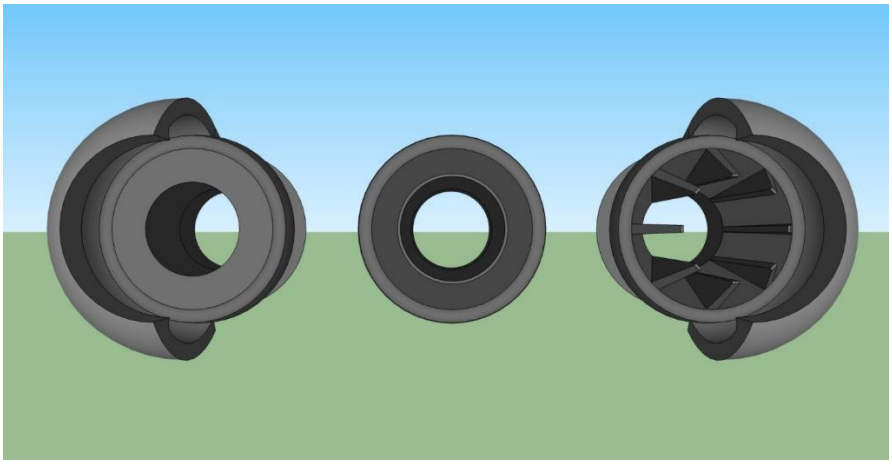

Figure 3: NIF MK. 1 - looking from the intake side

To ensure the applicability in different filtration needs, three variations of the Tunnel have been designed for the MK.1 prototype. The Standard Short Tunnel is found to be ideal for compact Cores, by offering a compact and efficient design. The Extended Tunnel is tailored for longer Cores, providing increased filtration capacity. For even more advanced needs, the Extended Finned

Tunnel is available, which is also designed for longer Cores but features an expanded surface area for enhanced air exchange. The diagram below (Figure 4) illustrates the working mechanism of the NIF MK.1, demonstrating how its static and mobile components interact.

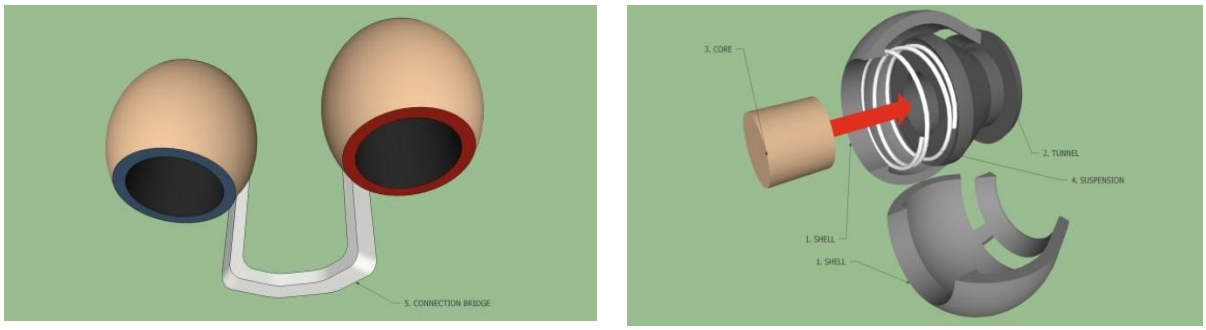

Figure 4: Interaction between parts of the NIF

During the inhalation phase, (Figure 5) the inhalation flow (represented by blue arrows) drives the mobile phase into the closed position, as depicted above. This action causes the tunnel to seal the air vents at the rear of the nasal filter, effectively directing the airflow through the central part of the tunnel, where the core filter is located. As the air passes through the tunnel, it is purified (Light blue arrows). The suspension in this case rebounds to secure the mobile phase in the closed position, with sufficient rebound force to maintain the mobile phase in place.

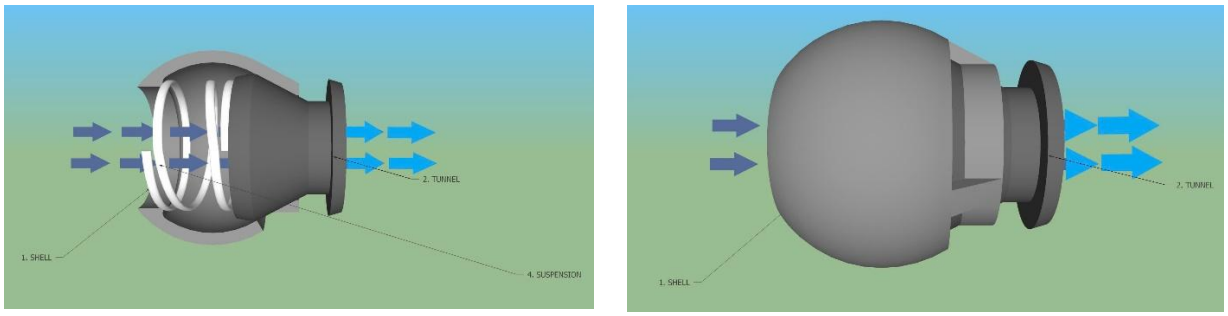

Figure 5: NIF during inhalation phase

During exhalation, (Figure 6) the exhalation flow (represented by red arrows) passes through the air vents, exiting the nasal filter without re-entering the filter. There are two primary reasons for the need of a secondary air passage: first, the exhalation pressure is stronger, and providing an unobstructed air passage enhances comfort for the user; second, the exhalation pressure could potentially dislodge the core filter, and the secondary air passage serves as a pressure relief mechanism to prevent this, given that the core filter is replaceable. The suspension rate must also

be sufficiently soft to allow movement of the mobile phase without creating unnecessary resistance. This requires testing (appropriate spring rate and rebound) to determine the optimal suspension setting.

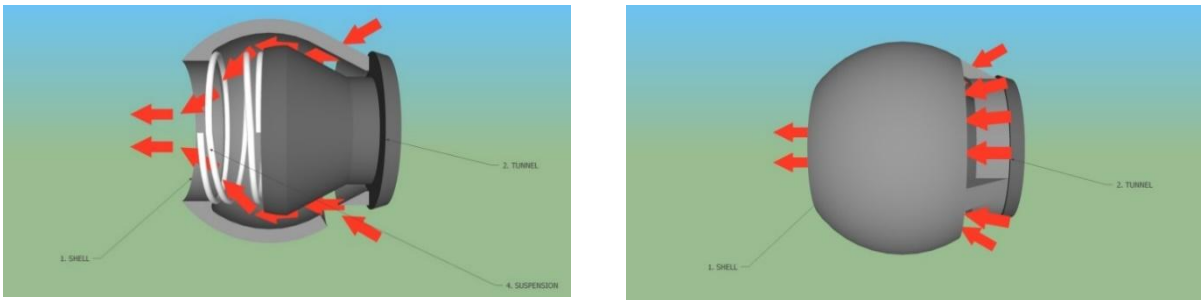

Figure 6: NIF during exhalation phase

Core – The heart and soul of this system, the core is a half-cone-shaped filter, which is a distinctive feature of the nasal filter's design. The core is replaceable, allowing users to purchase only the nasal filter body initially and replace the core when it is depleted. The old core can be easily removed and a new one inserted, enabling the user to keep the filter body while only needing to buy new cores. The half-cone shape of the core ensures it fits correctly into the tunnel. This design benefits both users and manufacturers: users only need to buy the body once, which is a high-quality product, while cores are relatively inexpensive. For manufacturers, selling cores provides a steady revenue stream, as demand for cores is consistent, with weekly or daily sales. Additionally, replaceable cores offer the advantage of interchangeability, meaning users can choose from various types, such as a standard dust filter or specialized filters like SYNFASAN G3. This provides both buyers and manufacturers with endless options. Three types of cores have been designed and will be detailed further in later sections. Suspension – The coil spring that keeps the tunnel in the closed position during inhalation, as discussed earlier, must have a spring rate soft enough to allow compression during exhalation while maintaining enough rebound force to keep the tunnel securely in place. Connection bridge – A thin yet incredibly strong bridge that connects and stabilizes the left and right nasal filter bodies, positioned just beneath the nose's bridge. The design of the initial prototype of the nasal filter incorporates several notable advantages. A key innovation is the two-ways airflow system, which ensures efficient air exchange. The device features interchangeable and replaceable cores, allowing for easy maintenance and customization to meet specific filtration needs. The chassis is robust and crafted from high-quality materials,

ensuring both strength and flexibility. Its ergonomic design includes a soft outer shell that conforms to the unique shape of each user's nasal cavity, providing a comfortable and secure fit. Aesthetically, the nasal filter is nearly invisible when worn, helping users feel more confident by avoiding unwanted attention. However, the design does present some challenges. The small diameter of the filters can reduce airflow, potentially making breathing more difficult. Additionally, the system's complexity may lead to higher production costs, which could raise the price and limit accessibility.

3.2. Design of the Nasal Internal Filter MK.2 (Mark 2)

To improve on the design of the first model, the MK.2's aim is to maximize the surface of air exchanging.

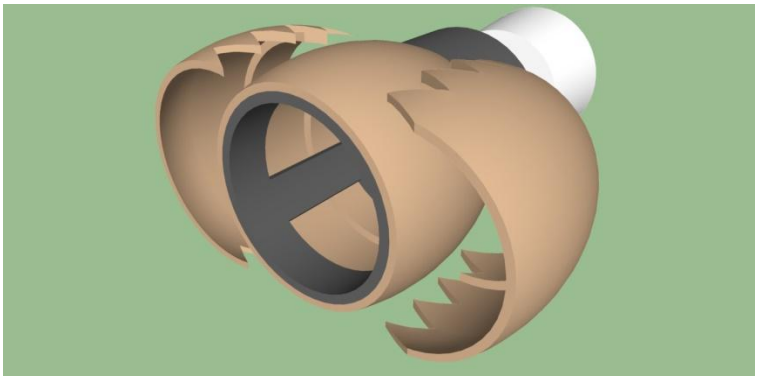

Figure 7: NIF MK.2 perspective view of parts

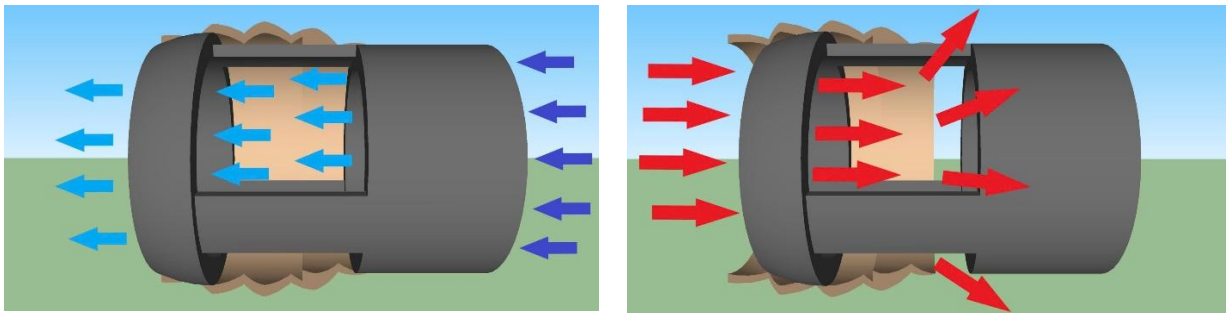

Figure 8: NIF MK.2 working mechanism

(Figure 8) During inhalation (Left panel) the tunnel is fully closed forcing the air to go through the filter core. During exhalation (Right panel) the tunnel is pushed forward to reveal 3 vents where the higher pressure expiratory air flow can escape easily.

The updated design incorporates a coil spring to enhance the mechanism's functionality. The spring's damper and rebound settings must be carefully calibrated to ensure optimal performance: the damper should be soft enough to allow air pressure to open the system, while the rebound must be firm enough to maintain its closed position. The coil itself is made from an ultra-thin yet durable stainless steel filament, finer and thinner than a typical ballpoint pen spring but produced using a similar manufacturing process. A notable addition in the new design is a railing frame, represented by the gray component, which guides the mechanism's movement. This frame is crafted by folding thin, pressed metal sheets into a tubular shape, requiring an extremely precise and delicate manufacturing process. The material must be strong enough to resist deformation while also being capable of collapsing safely in the event of an impact, such as accidental nose trauma while wearing the filter. This collapsible feature ensures that the shell remains intact to prevent sharp fragments from entering the nasal cavity or respiratory tract, thereby minimizing potential risks. The MK.2 design offers a significant advantage by maximizing the surface area for air exchange. The tunnel frame's diameter has been expanded to optimize airflow efficiency. However, some challenges persist. The thinner tunnel construction makes it more fragile than the original model, and the increased design complexity could pose manufacturing difficulties. Additionally, the presence of protruding moving parts may be distracting or uncomfortable for the user.

3.3. Design of the Nasal Internal Filter MK.3 (Mark 3)

The model MK.3 serves as an effective compromise between the previously designed first and second nasal filter systems. according to the observations it combines the larger diameter filtering tunnel of the second system while keeping all moving parts enclosed within the shell, eliminating any potential distractions for the user.

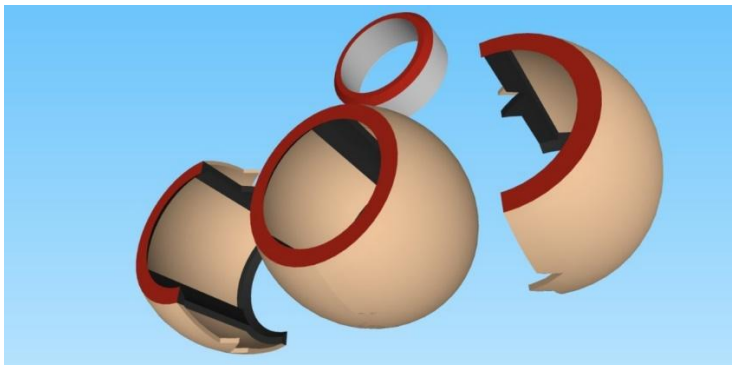

Figure 9: NIF MK.3 perspective view of parts

(Figure 10) During inhalation (left panel), the tunnel is pushed into the closed position, forcing air to pass through the filter. During exhalation (right panel), the tunnel moves forward to approximately the middle section of the shell, allowing the high-pressure expiratory airflow to travel over the dome of the shell and exit the system through designated channels.

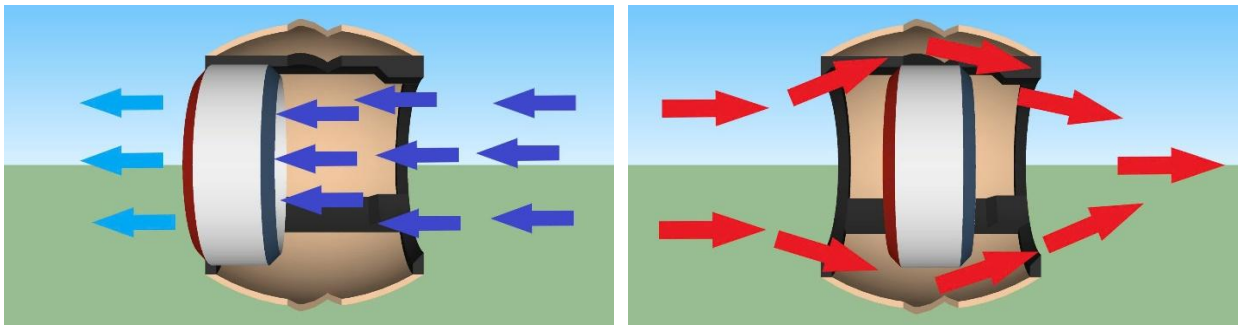

Figure 10: NIF MK.3 working mechanism

A coil spring is used to maintain the mechanism. The MK.3 strikes a good balance between comfort and aesthetics, offering an elegant yet practical design. While it is no more challenging to manufacture than the MK.2, it shares similar levels of fragility and complexity.

3.4. Design of the Nasal Internal Filter MK.4 (Mark 4)

The MK.4 is the simplest model to produce so far, with a primary focus on the replaceable filter function. Its mechanism of action involves a pin that secures the filter within the shell. To replace the filter, the user simply pulls out the pin and inserts a new filter. The main advantages of this design include simplified manufacturing and the potential for smaller sizes, making it suitable for children. However, its limitation lies in the restricted range of compatible filter cores, which are primarily sheet or membrane filters.

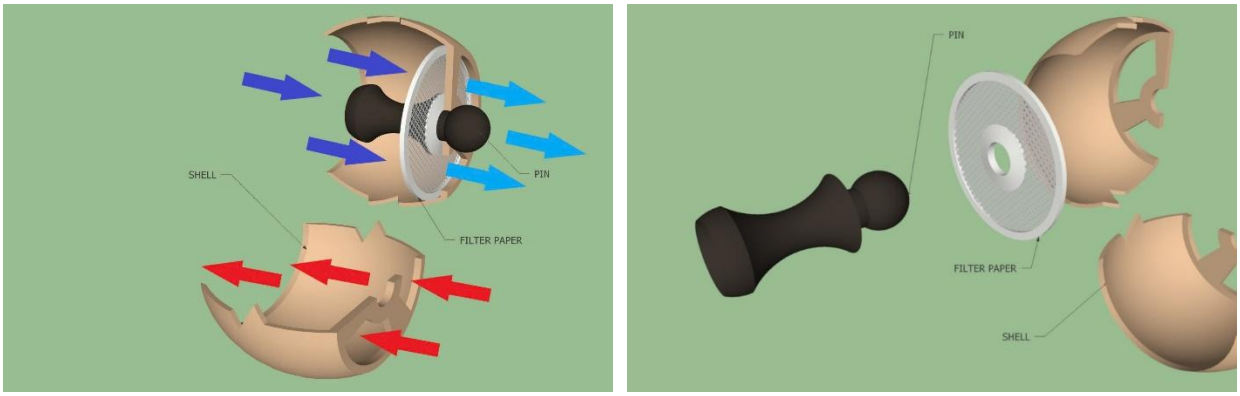

Figure 11: NIF MK.4 parts diagram

3.5. Design of the Nasal Internal Filter MK.5 (Mark 5)

The NIF MK.5, designed in 2018, builds on the best features of the previous models. While retaining the same principles as the original MK.1, this new design achieves optimal simplicity and efficiency. The system consists of only four parts—left shell, right shell, coil spring, and filter core—compared to six parts in the MK.3, streamlining the manufacturing process.

The MK.5 also features the largest filter surface, comparable to that of the MK.2. Its design was inspired by the mechanics of Birome's ballpoint pen, which is reflected in its name. Alongside the NIF MK.5, the MK.5 stands out as one of the simplest and most durable systems developed so far. With its streamlined construction and robust design, the MK.5 has the potential to be the most effective of all models, particularly in its application of the two-ways airflow mechanism principle.

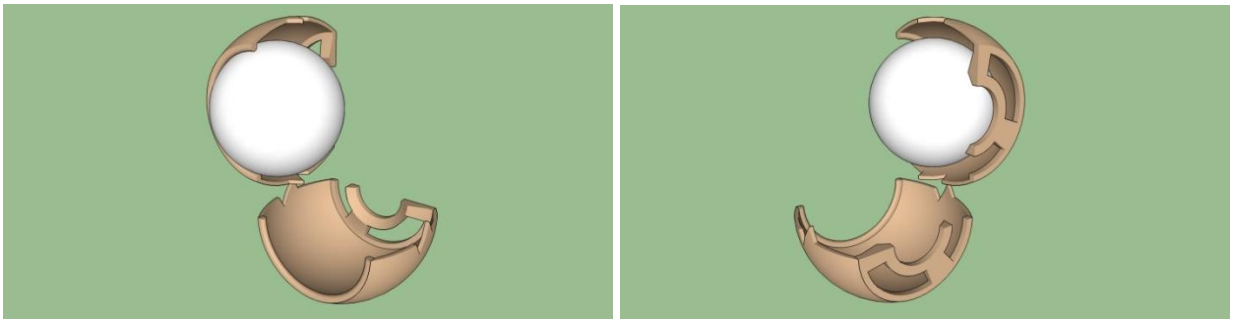

Figure 12: NIF MK.5 parts diagram

Figure 13: NIF MK.5 working mechanism from the inside

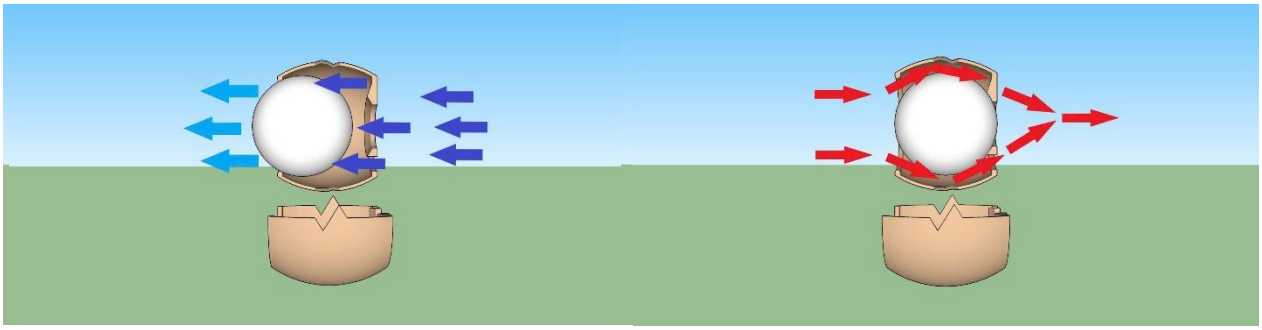

Figure 14: NIF MK.5 working mechanism from the outside

MK.5 filter core is ball shaped, there is no complicated housing or railing system, the filter is polymer-matrix type so it is very versatile. The ball core manufacturing process is similar to that of other normal filter, just the mould is round. Also like the previous models, user can change the Filter by punching the old one out and just by their hand push new one in.

NIF Generation	Advantage	Disadvantage
MK.1	First concept: introduces two-ways airflow mechanism, shell shape, replaceable filter	Very complicate Lot of moving parts Small filter surface
MK.2	Two-ways airflow Large filter surface Replaceable filter	Very complicate Lot of moving parts Aesthetic concern
MK.3	Two-ways airflow Large filter surface Replaceable filter	Very complicate Lot of moving parts
MK.4	Two-ways airflow Large filter surface Replaceable filter 1 moving part	Complicate Filter choice restricted Filter replacement difficult
MK.5	Two-ways airflow Highest filter surface Replaceable filter Simplest design 1 moving part	

Table 1: Summary table for NIF Generations

Several test iterations have identified the MK.5 model as the most suitable for FDM 3D printing, primarily due to its structural simplicity. This design allows for the theoretical fabrication of a full-scale, functional prototype by 3D-printing the more intricate components of the shell, while supplementary parts can be manually integrated post-production. Experimental Prototype 1 (XP1) was printed using PLA filament. This early real size 3D print design was of NIF MK.1 mainly to test feasibility of connection bridge and clamp (Figure 16).

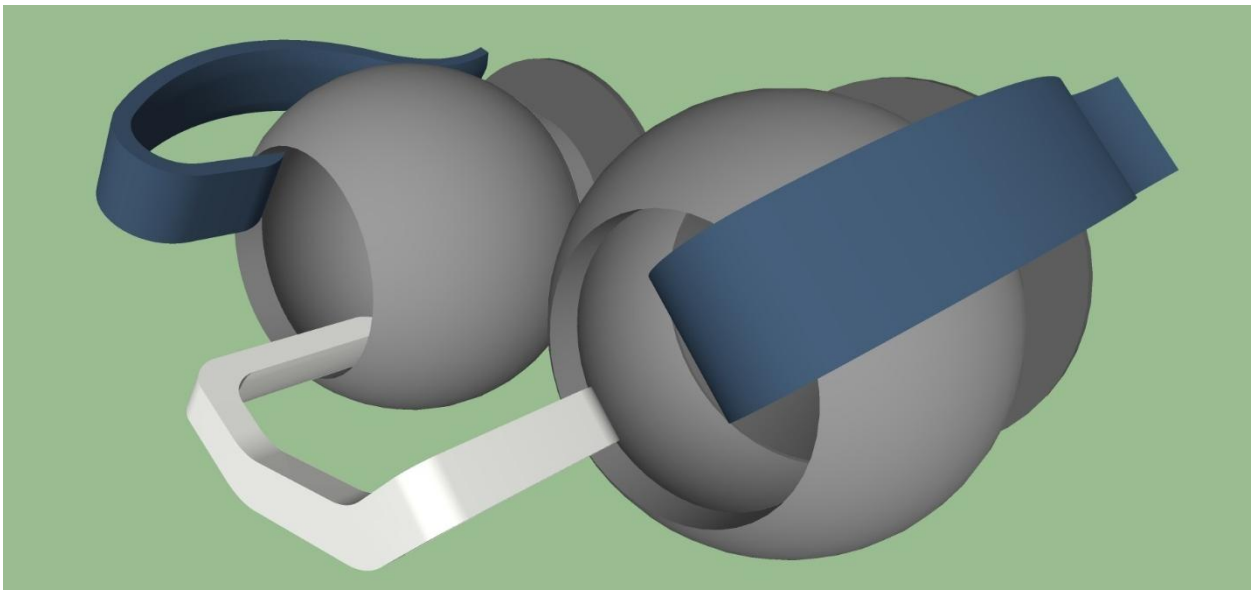

Figure 15: MK.1 XP1 original print design with full bridge and clamp

Figure 16: MK.1 XP1 after print

The clamps were deemed unnecessary due to several complication in removing the parts moreover they broke easily. According to this finding design was simplified to just connection bridge, subsequence clampless design were designated with E1 (Evolution 1) (Figure 18).

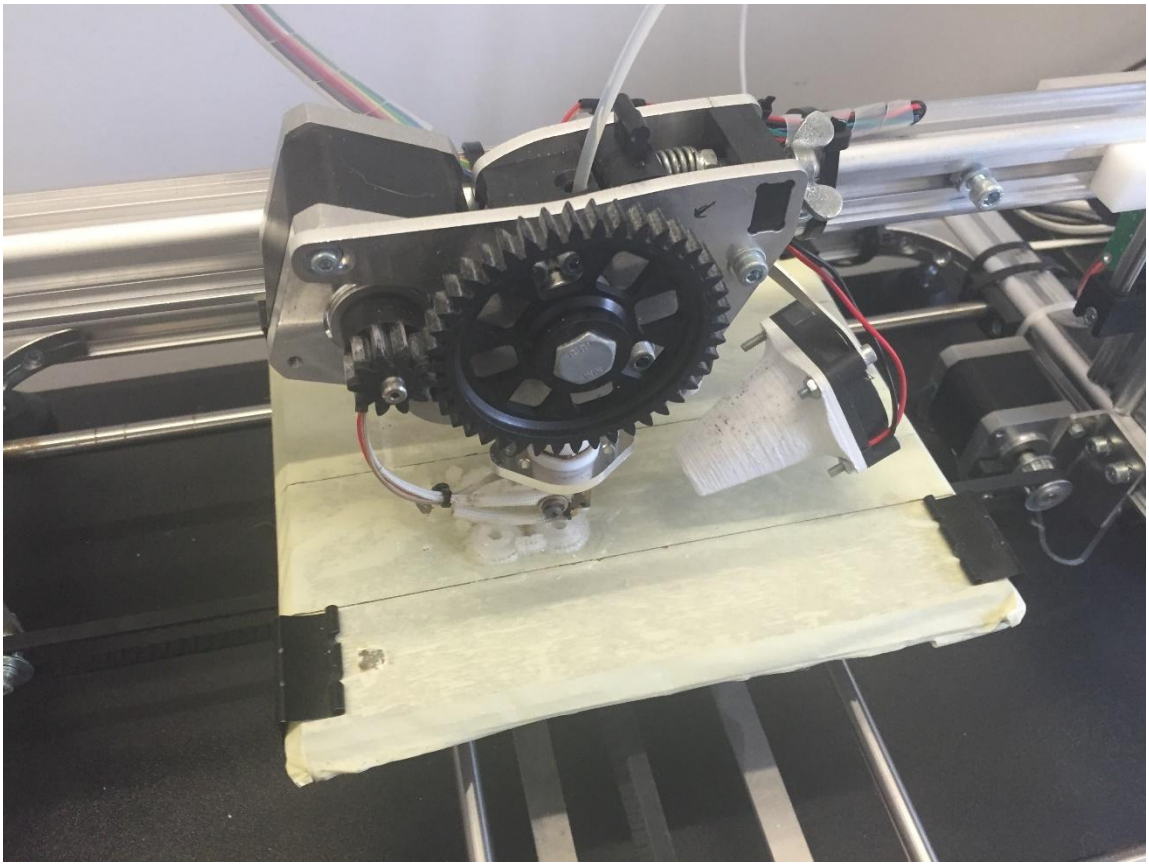

Figure 17: 3D Printer working on NIF

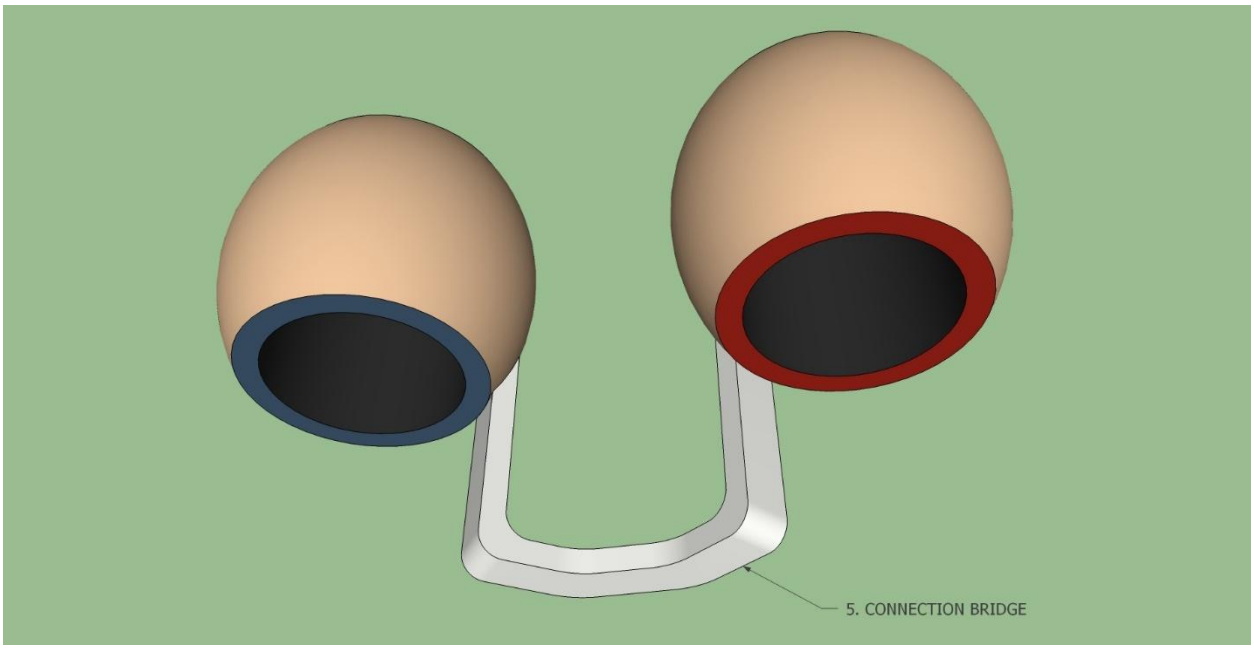

Figure 18: 3D NIF MK.5 E1 print design

At the time this design was decent and more importantly our 3D Printer can realistically work with it. Noticeable details: left shell is marked with red color while blue indicates right shell, bridge faces down. At this point the device is inflexible due to its fixed orientation.

Figure 19: NIF MK.5 XP1 E3 After print

4. ASSESSMENTS AND PERFORMANCE TESTS

Following the completion of XP1 printing, assessments and performance tests were conducted to evaluate the mechanical strength of different NIF bridge designs and the structural integrity of the case using a Brookfield texture analyzer. Three prototypes, each featuring distinct bridge designs—E1, E2, and E3—were fabricated using a Craftbot 3D printer and PLA as the primary material. The aim was to determine which bridge design offered the best mechanical performance under physical stress. The prototypes were prepared under different 3D printing configurations. For E2 and E3, the printing parameters included a top-to-bottom layer ratio of 8:10 without vase mode, a raft offset of 3 mm, and auto-generated support structures.

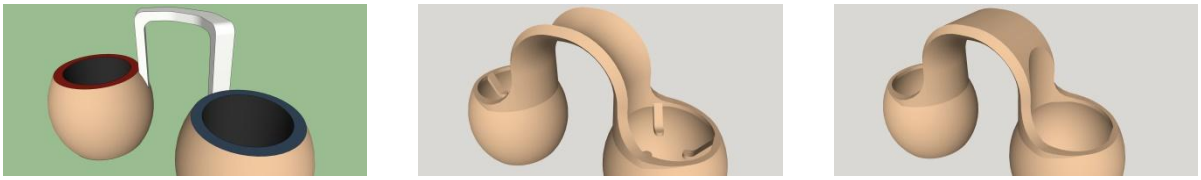

NIF MK.5 XP1 E1 NIF MK.5 XP1 E2 NIF MK.5 XP1 E3

Figure 20: NIF MK.5 XP1 Evolution differences

E2 demonstrated superior mechanical performance in the evaluations, moreover E3 outperforming the results in the aspect of resistance to impact and durability. E2's enhanced performance is attributed to its thinner bridge design, which allowed for greater flexibility, enabling it to absorb more energy before structural failure. E3, despite its thicker structure, exhibited lower tolerability due to its limited ability to withstand bending. Once the mechanical threshold was surpassed, E3 failed more catastrophically than E2. These observations align with the mechanical behavior of PLA, a material known for its rigidity and limited elastic properties. Notably, errors during the conversion of 3D models to the Craftbot printer led to minor defects in the test prototypes, which may have influenced the results. These issues were later rectified, ensuring the accuracy of subsequent analyses. The case structure made from PLA exhibited good resistance to cracking, tearing, or splintering during testing. However, under significant force, the case collapsed and retained a permanently deformed shape, confirming that PLA does not meet the material requirements for this application due to its lack of resilience under compressive stress. In conclusion, the E2 bridge design was determined to be the most suitable for subsequent prototypes due to its optimal balance between flexibility and strength. This design offers improved structural

performance and ensures greater reliability under physical stress. Future developments will focus on refining the prototype further to enhance its mechanical properties and overall functionality.

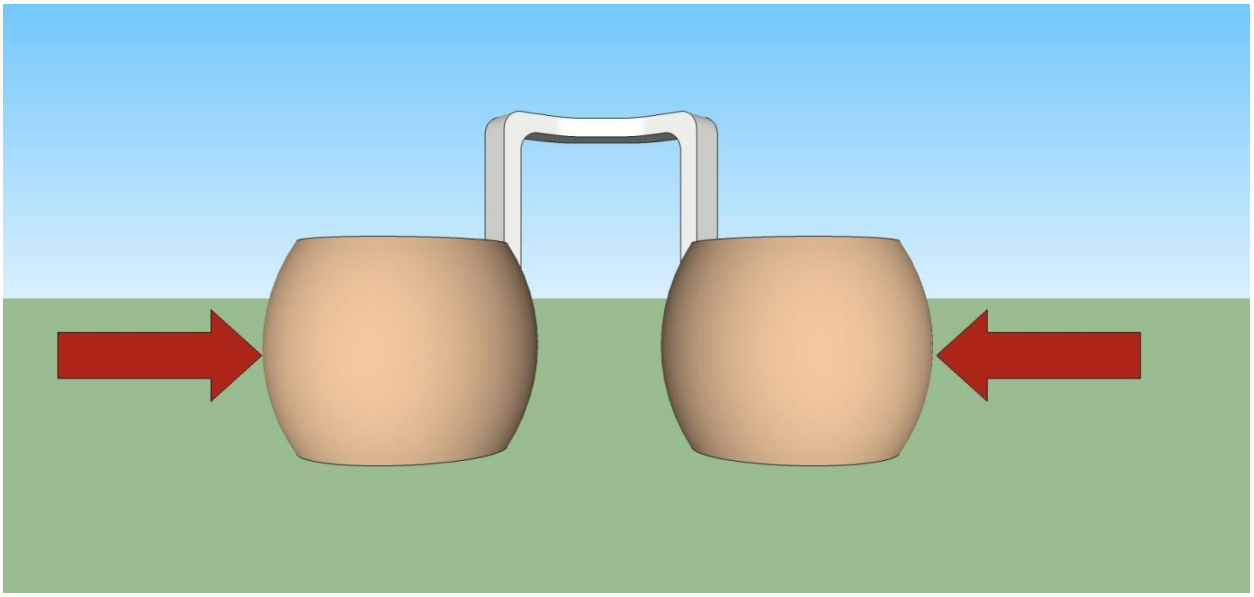

Figure 21: NIF MK.5 XP1 compression direction during Brookfield CT3 texture analyzing

Tests were conducted by volunteers regarding the applicability of the prototype.

Type	Shell diameter (.00 mm)	Bridge height (.00 mm)
NIF MK.5 XP1 XL	10.50 mm	10.50, 09.45, **08.40**, 07.35
NIF MK.5 XP1 L	10.00 mm	10.00, 09.00, **08.00**, 07.00
NIF MK.5 XP1 M	09.50 mm	09.50, 08.55, **07.60**, 06.65
NIF MK.5 XP1 S	09.00 mm	09.00, 08.10, **07.20**, 06.30
NIF MK.5 XP1 XS	08.50 mm	08.50, 07.65, **06.80**, 05.95
NIF MK.5 XP1 XXS	08.00 mm	08.00, 07.20, **06.40**, 05.60

Table 2: NIF MK.5 XP1 interested size dimensions

During the test, volunteer staff members—comprising an approximately equal distribution of men and women aged 22 to 50 evaluated the prototypes primarily based on comfort.

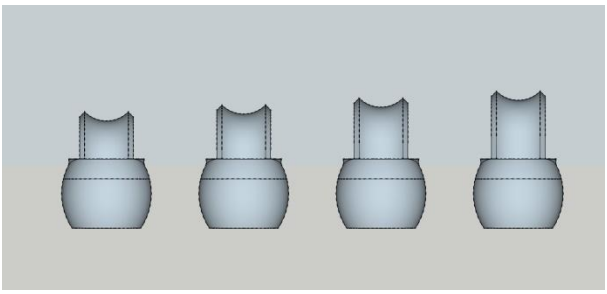

Figure 22.: Bridge height differences

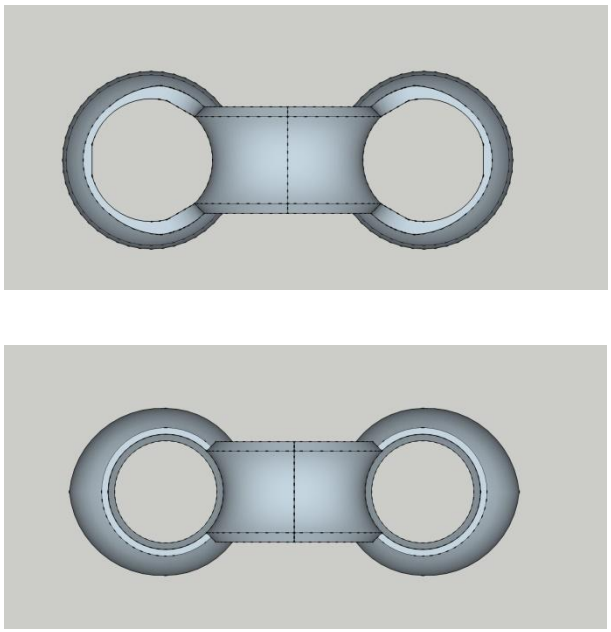

Figure 23: NIF MK.5 XP1 (Upper) vs XP2 (Lower)

All nasal filters produced for this test were NIF models without a suspension component, aimed solely at evaluating fit and comfort. All models featured symmetry along both the frontal and horizontal planes for simplified production, with size differences set at a 5% increment, such that MEDIUM equaled 95% of LARGE. Common feedback indicated that the bridge on all XP1 models was too high, causing the housing to extend too far into the nasal cavities, leading to asymmetrical fitting issues where one side sat deeper than the other, poor air sealing, and chafing when speaking. (Figure 22) To address this, models labeled -1(09.00 mm), -2(08.00 mm), and -3(07.00 mm) featured progressively reduced bridge heights in 1 mm increments for size LARGE, with the best results obtained from -2 and -3: -2 offered more flexibility and looser tolerance, while -3 provided a snug fit and avoided chafing during speech but was less flexible. On first use, most participants described an alienated feeling, stating that it felt like a foreign object but might improve over time. After two hours of wearing the NIF MK.5 XP1 LARGE-2, the filter became less noticeable, though contact or movement in the nasal area triggered the foreign-object sensation again. The XP1's shape also did not ensure a tight fit, posing a risk of falling out. These issues were resolved with the updated XP2 model, which fit naturally and securely upon first use, and after extended wear felt almost imperceptible, although further improvements could be achieved

by using softer materials and refining the surface finish. Additionally, in response to requests from several female users, the XP3 model was developed as an upward-rotated version of XP2, providing better alignment that raised the nasal profile, a feature favored by many female participants. Based on these results, the XP2 model will serve as the basis for subsequent designs. For a full-scale working prototype, the NIF MK.5 XP1 was selected as the foundation for Validating Prototype 1 (VP1). It was determined early in development that the NIF MK.5 filter stopper could not be feasibly produced using 3D FDM printing, and large-scale manufacturing posed significant challenges, prompting the creation of several new designs to address these issues.

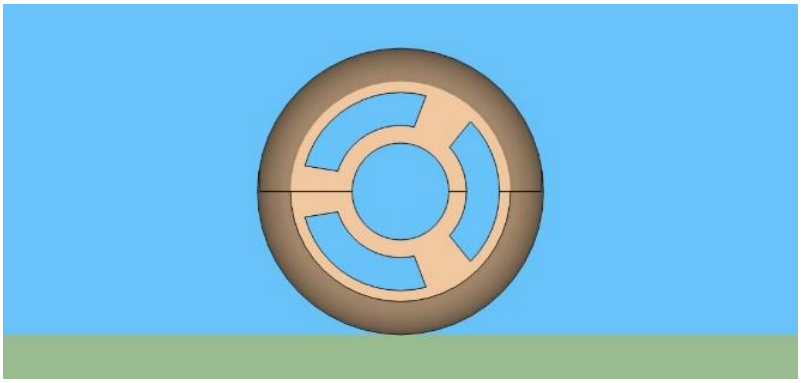

Figure 24: NIF MK.5 XP1 VP1 filter stopper

4.1. NIF VP2

VP2 can be printed using an FDM 3D printer, and in theory, the stopper for VP2 would be manufactured from the same elastomer material as the shell. This design allows the stopper to be flexible and mimic the original suspension mechanism intended to keep the filter in a closed state during breathing. However, the physical properties of the stopper were found to be unsatisfactory, as it proved to be very weak and prone to breakage, often failing simply during the removal of the NIF from the printer's bed.

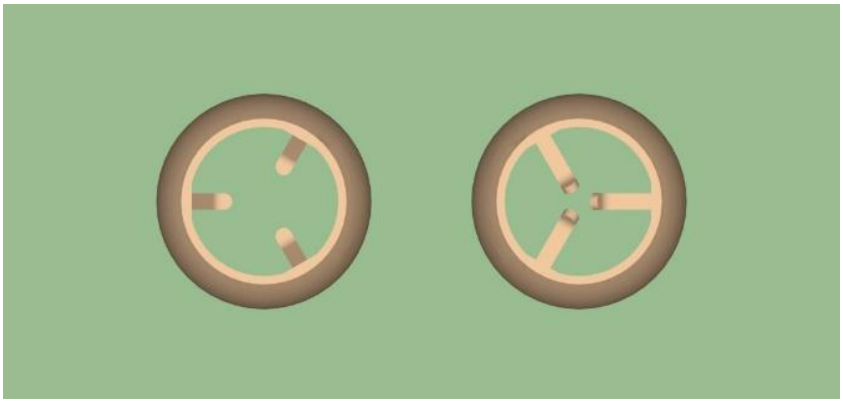

Figure 25: NIF XP1 VP2 prong filter stopper

4.2. NIF VP3

The VP3 stopper featured a beefier and simpler design that could be 3D printed, but it exhibited significant stringing due to the bridging length exceeding the machine's capabilities. Consequently, the suspension mechanism initially intended for the NIF was abandoned, as in vivo testing with the G3 filter demonstrated that the filter could remain in a closed state purely through inhalation pressure.

The stopper's revised role was limited to preventing the filter from being ejected and maintaining an appropriate gap to relieve exhalation pressure. The VP3 stopper was strategically positioned to meet these new functional requirements.

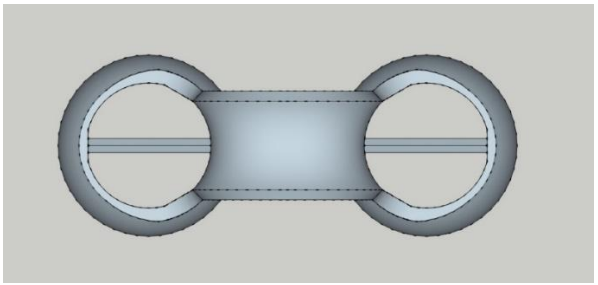

Figure 26: 3D model of NIF XP2 VP3

4.3. NIF VP4

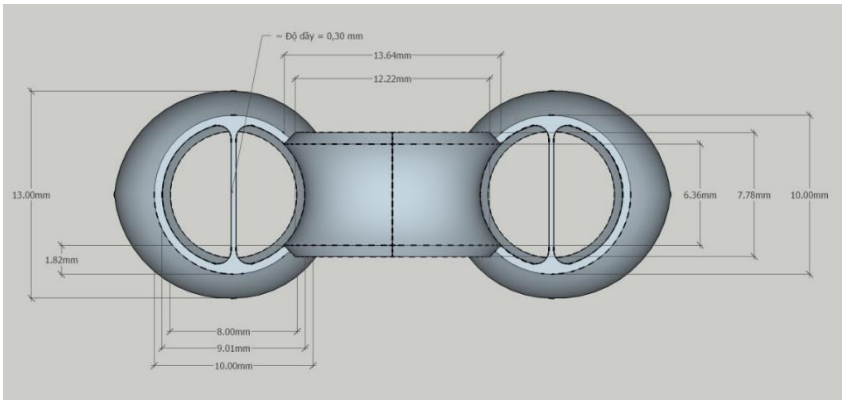

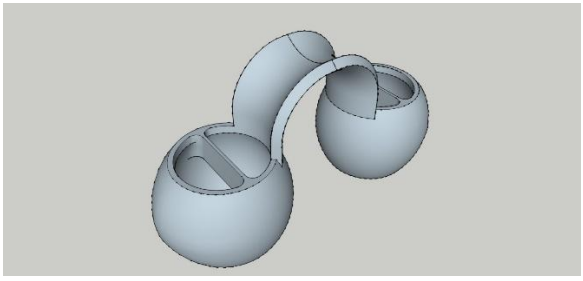

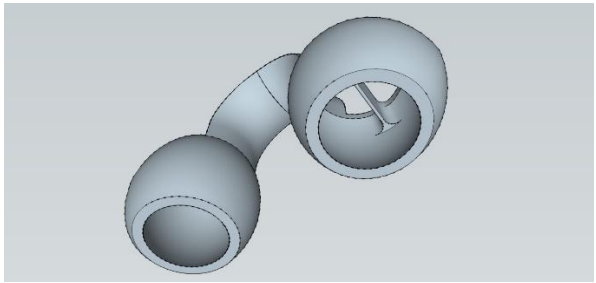

Figure 27.: 3D model of NIF XP2 VP4

The VP3 stopper, positioned horizontally, proved unfavorable under applied physical force, as this design restricted structural flexibility and compromised lateral compression resistance. To address

this issue, the VP4 stopper was reoriented to a vertical position (Figure 27), enhancing its structural integrity and performance.

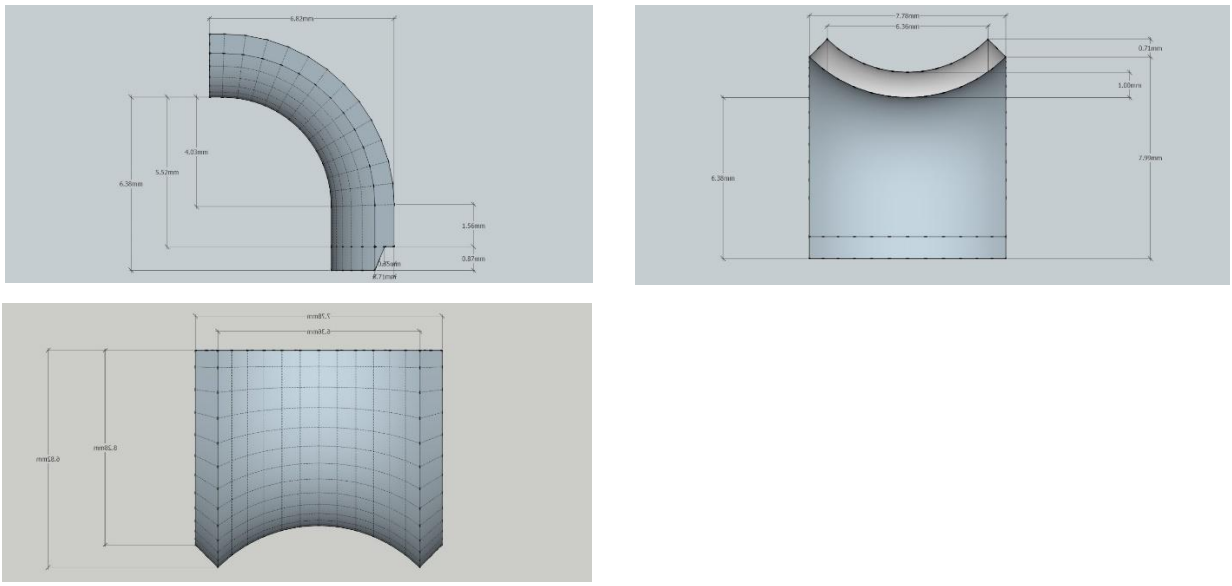

Figure 28: NIF XP2 VP4 size L Bridge Dimensions

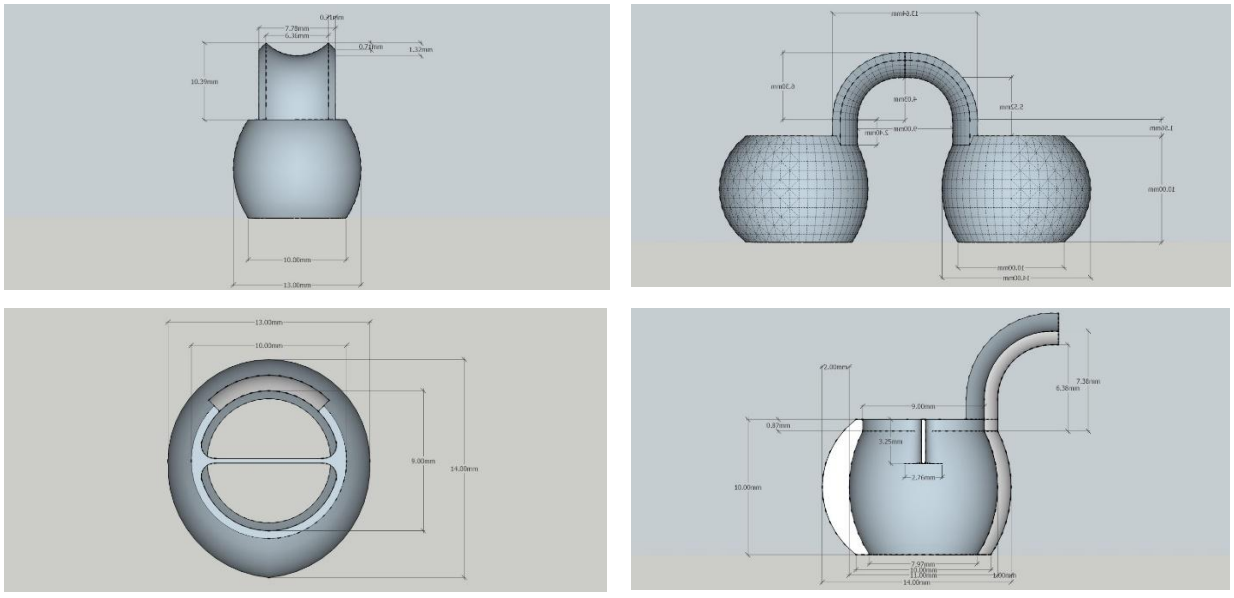

Figure 29: NIF XP2 VP4 size L - side and shell dimensions

The stopper will be excluded from the printing process and instead will be cut and glued separately. Initially, only the XP2 main shell will be printed, followed by manual preparation of its surface.

The stopper is cut from a plastic sheet into a specific shape, fitted, and glued onto the prepped XP2 shell. The assembly is then allowed to cure for a minimum of 12 hours to ensure the removal of all adhesive vapors. Subsequently, the VP4 prototype will undergo a chemical disinfection process using a 70% ethanol solution. Further details of this process are outlined in the subsequent sections of the dissertation.

Design was tested fit into the nose on *Figure 30*

Figure 30: Position of NIF when observed from the front

5. FDM TECHNOLOGY, 3D PRINTING, AND ITS COMPONENTS

5.1. Foundations of instrument development

The CraftBot3 3D Printer (model discontinued) is a high-performance 3D printer designed for precise and efficient printing with a variety of materials. It features two direct drive independent extruders (IDEX), allowing for dual-material printing and improved print quality, particularly when using soluble supports. The printer offers a substantial print size of 374×250×250 mm, making it suitable for a wide range of applications from prototyping to functional parts production. Key specifications include a layer resolution ranging from 50-300 microns, providing excellent detail for both fine and larger prints. Its positioning precision is 4 microns on the XY axis and 2 microns on the Z axis, ensuring high accuracy in printed objects. The filament diameter is 1.75 mm, compatible with a wide range of filament types. Nozzle diameter is adjustable between 0.25-0.8 mm, offering flexibility in printing resolution and speed according to the manufacturer suggestions. The applied temperature can be also adjusted between 180°C and 300° Celsius, enabling the use of various filaments such as PLA, ABS, PET, and more. The bed temperature can be ranges from 50°C to 110°C, making it ideal for different materials and ensuring proper adhesion during printing procedure. The print speed ranges from 50-200 mm/s, providing a balance between quality and speed. It is capable of handling a wide variety of materials, including PLA, ABS, PVA, PET, HIPS, Nylon, and more, making it a versatile tool for different applications.

Figure 31: Craftbot 3 FDM printer – Hungarian made

5.2. Applied Filaments for FDM printing

5.2.1. MD1 FLEX

MD1 Flex is the first applied filament for the manufacturing process. It is an innovative nanocomposite filament developed by Copper3D. The MD1 Flex filament combines high-quality TPU98A with a patented nano-copper additive, resulting in a unique material that not only maintains the mechanical properties of TPU98A but also incorporates powerful antimicrobial features. The integration of this nano-copper additive makes MD1 Flex highly effective in eliminating a broad range of microorganisms, including fungi, viruses, and bacteria. These antimicrobial properties make MD1 Flex particularly suitable for medical applications, such as our development and in all areas where hygiene and infection control are extremely important. MD1 Flex retains all desirable mechanical properties of TPU98A, including hardness, flexibility and exceptional elongation at break, reaching 450%. In addition to all this, the filament also shows impressive heat resistance, withstanding temperatures up to 138°C. This makes MD1 Flex the ideal material for applications that require durability and high performance under stress. In addition, the filament is highly compatible with 3D printing technologies, allowing print speeds of more than 75 mm/s without compromising quality or performance. The filament is versatile, so it is also used in the production of many other medical devices. In addition to medical use, MD1 Flex has significant potential in many other industries that require high-performance, antimicrobial materials.

5.2.2. PLA

Poly Lactic Acid is a widely used filament for Fuse Deposition Modeling. It is easy to be printed, is rather weak against mechanic force; has very slight flexibility, biodegradable, dissolves in Acetone, glass transition temperature at 60°C - printed structure can warp in contact with ex. boiled water. The most important parameter for PLA is printing temperature, there are no set temperature setting for each filament, but it is a range and depending on each combination of 3D printer + brand of filament, the temperature setting is different. For PLA filament the preferred temperature setting (Craftbot3) is: print head at 200°C and print bed at 60°C. Print speed for best quality is 30 mm/s and max is at 60 mm/s for an acceptable result; lower than 30 mm/s does not improve quality much and above 60 mm/s will make a mess. PLA can work with fine 0.25 mm printer nozzle so

model definition quality is high. Polylactic Acid (PLA) is a widely used thermoplastic material known for its rigidity and moderate tensile strength. While PLA exhibits intermediate strength properties, it is prone to breakage under slight crushing forces, with the fracture typically occurring at the interface between printed layers. This is because the individual strands of PLA do not form direct bonds across layers, leading to a weakness at these junctions. However, PLA demonstrates good shear strength, meaning that forces exerted along the length of a strand do not easily cause it to break. Instead, such forces tend to permanently deform the material, provided the shape has already set. The strength of 3D printed products produced with PLA material is influenced by many factors, including the structural design of the intended object, the physical location of the print in the 3D printer, and the parameters of the printing process used. One of the most well-known properties of PLA is its thermoplastic nature, which allows the material to melt and reshape. However, it is a known fact that without consequences, this process can be repeated no more than three times before the substance begins to decompose. After several remelting cycles, PLA becomes brittle and crispy, making it unsuitable for further use. Although PLA is a relatively fast and easy-to-use filament, its mechanical properties and tendency to degrade after multiple conversion cycles make it unsuitable for certain applications, such as the nose filtration system.

5.2.3. TPU

As a sided elastomer polymer, thermoplastic polyurethane (TPU) is clearly renowned for its flexibility, durability and flexibility. For 3D printing jobs, TPU is available in different hardness levels. The MD1 Flex version with a shore hardness of 98A contains a patented nano-copper additive. This property greatly improves its antimicrobial properties and makes it suitable for both medical and food applications. The TPU's inherent flexibility also makes it ideal for applications requiring comfort and durability, such as prosthetic devices, accounting for approximately 70% of applications. Parts printed with TPU 98A show significantly higher strength than those made of classical PLA. Based on these, it can be concluded that they can withstand higher mechanical stress without breakage. However, printing with TPU presents significant challenges in many cases. The material has hygroscopic properties. This can clearly adversely affect print quality. So it can be said that TPU, especially the MD1 Flex version, offers a combination of flexibility, durability and antimicrobial properties. This makes it suitable for applications that require high precision and

biocompatibility. Although working can present printing challenges, adherence to specific storage and printing protocols can alleviate these issues, resulting in high-quality, functional prints.

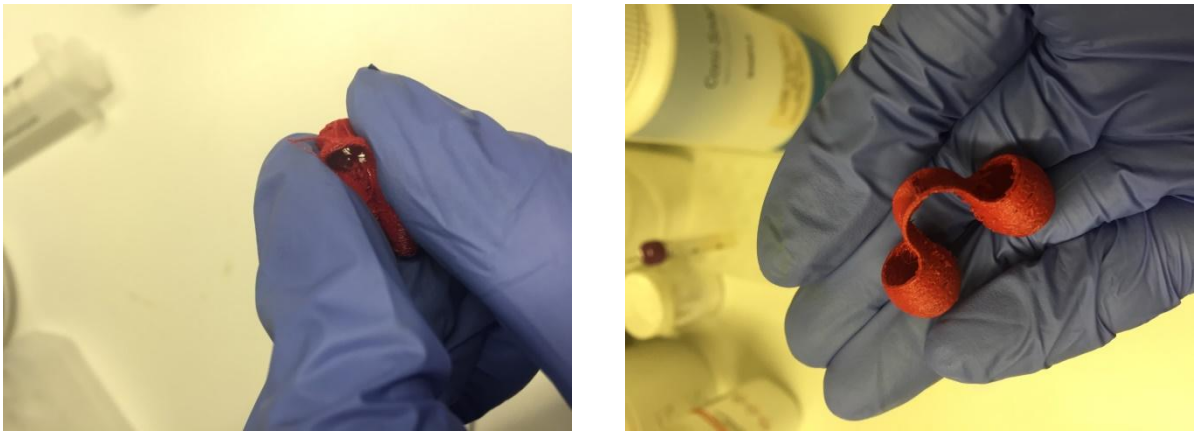

Figure 32: Printed prototypes from TPU

Despite the many advantages listed, it must be acknowledged that TPU has its own challenges, especially during the printing process. We have also experienced this in our experiments. The material is sensitive and very accurate in hardware settings and software settings. One important aspect is its hygroscopic nature, which was mentioned earlier. This can clearly negatively affect print quality. If the filament is too wet, the print head may make popping sounds during operation, which is not a big problem in itself, but the final print may show stringing, which is a very common problem with TPU. This becomes even more pronounced with increased humidity. To prevent these problems, it is essential to store the TPU in a vacuum-sealed bag with desiccant. However, this is not always killable, nor is it a sure solution in many cases. To solve the stringing problem, setting the Z-hop setting to 0 mm/s can help by preventing the 3D print head from moving while moving, thus reducing unnecessary string formation. Clearly speaking, printing using TPU clearly requires a certain level of experience and patience, as slower print speeds are required for optimal results. As an advantage, the temperature settings of TPU printing are relatively flexible as long as they fall within the recommended range specified by the manufacturer. A typical temperature setting would be around 215°C for the print head and 60°C for the print bed. Importantly, unlike PLA, TPU's flexible nature allows it to adhere better to the print bed, and small parts usually do

not require additional glue. However, larger prints may still require a thin layer of adhesive to ensure secure bed adhesion, preventing possible warping or detachment during the printing process. Despite these challenges, TPU's flexibility and durability make it an excellent choice for many applications, especially those that require high mechanical strength and comfort.

5.3. Applied Software for design

For the design method Craftware PRO Premium has been applied. It is an advanced slicing software designed for FDM 3D printers. The program offers enhanced features for improved productivity. It was important for us during the selection that this software supports multi-device operation, provides advanced strategies for optimal print quality, and includes tools for faster printing with reduced manual interventions.

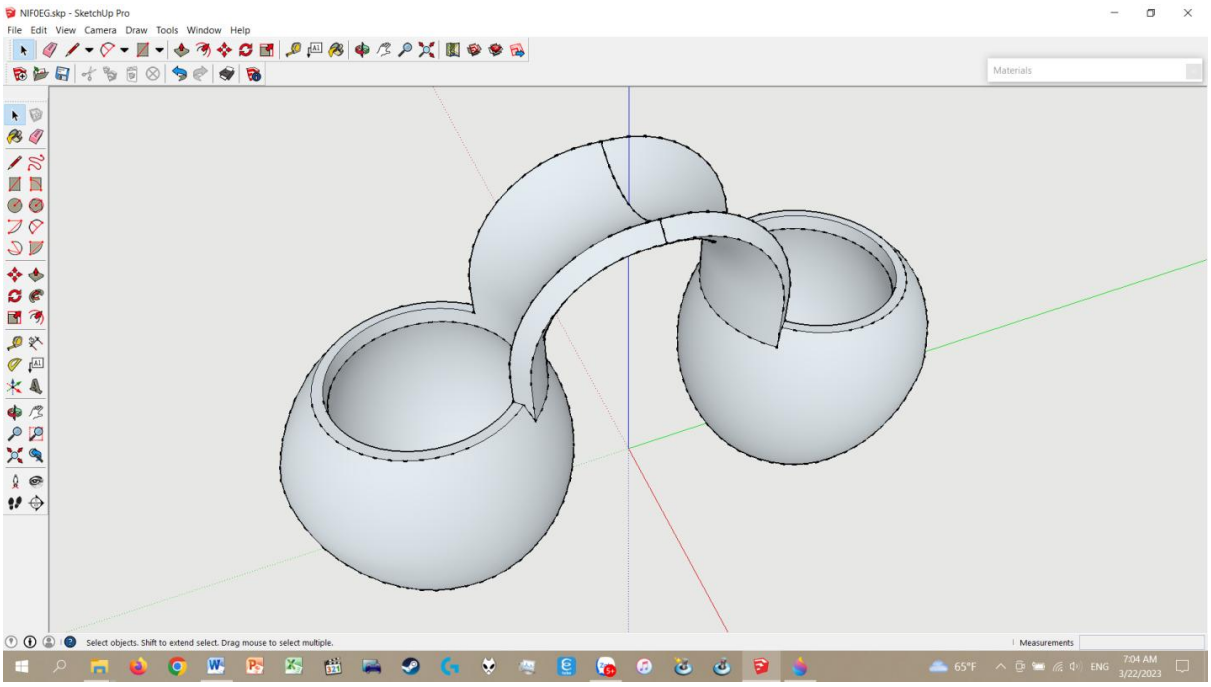

Figure 33: 3D model of NIF XP2 in SketchUp Pro

According to our observations, succesful aplication of Craftware PRO Premium for FDM 3D printing, based on configuring the printer settings, selecting appropriate slicing strategies, adjusting layer height, infill patterns, and support structures. The software allows optimization of print speed and quality through advanced settings such as multi-tray support and adaptive strategies. Proper calibration of print parameters, including temperature and material types, is

essential. Finally, previewing the slicing results to detect potential issues before printing is critical for ensuring high-quality output.

Figure 34: NIF XP2 VP5 working prototype

According to our observations it can be concluded that during the manual fabrication of VP4's item straight stopper, minor inaccuracies in cutting—particularly in components with longer dimensions—resulted in stoppers with a slight curvature. Interestingly, testing revealed that these curved stoppers outperformed their straight counterparts. The curved design exhibited improved vertical compression characteristics, with a predetermined angle of compression offering greater predictability. Furthermore, the manufacturing process was simplified, as the lower tolerance requirements facilitated easier production (See curved stopper from *Figure 34*).

6. NEF DESIGN AND PROTOTYLE PRODUCTION

The Nasal Emergency/ External Filter (NEF) is a two-part system. The main components are main housing and a removable filter core. During the design process, we considered it a priority to provide maximum nose protection while maintaining ease of manufacture. In essence, the NEF acts as a compact gas mask in an easy-to-carry pocket and is ready for immediate use in situations where subtlety or aesthetics are a secondary consideration, such as in smoke-filled environments or during a tear gas attack. This versatility and these hypothetical situations justify the term "emergency" filter. In addition, during development, our goal was to create a device that can be used effectively under a standard surgical or cloth mask, offering greater comfort and breathability compared to the smaller nasal internal filter (NIF) shown earlier. The main housing of NEF is made of flexible polymer, which is molded into an exact shape with a designated core channel and opening path.

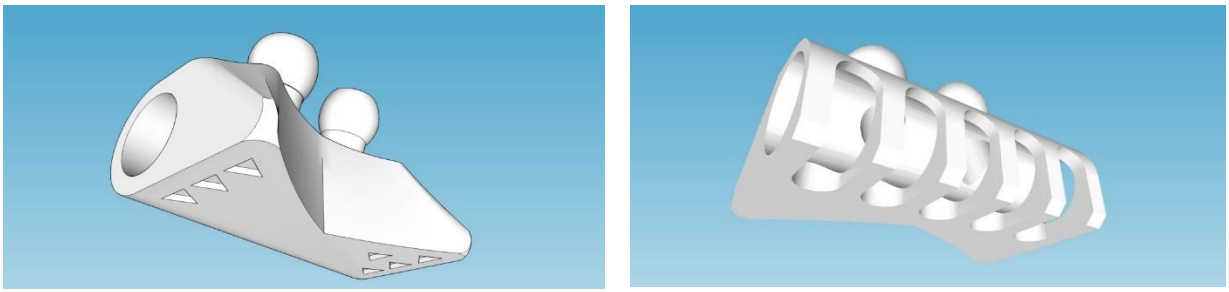

Figure 35: NEF MK.1 XP2 (left) and NEF MK.2 XP2 (right)

The filter core of the NEF is inserted into the channel, while the orifice pathway facilitates airflow between the filter and the nasal cavity. The core replacement process is notably more straightforward than that of the NIF. The filter cores themselves are constructed as matrix or layered systems, designed in a cylindrical shape for easier insertion and secure fitting. Development of NEF began in 2014 and continued beyond 2018, the latest model being the NEF MK.1 XP2. Currently, this version can be considered the "final" prototype. The NEF MK.2 is a lighter version with a more complex design to optimize airflow compared to the simpler tubular duct of previous models. Since then, all NEF MK.2 units have been upgraded to the XP2 variant, which significantly improves the efficiency of air exchange by integrating additional vents on its surface. Importantly, all NEF filters are interchangeable between models, and both the NEF

housing and its cores can be conveniently packed together for ease of use and storage. This adaptability and modular design highlights the practicality and effectiveness of NEF as a versatile respirator.

6.1. Applied filter for NEF

For the NEF system, a SYNFASAN G3 filter was used. It is a highly efficient and versatile filter material that is widely used in various industrial and commercial applications due to its durability and exceptional performance. The filter class G3 according to EN 779 standards and ISO coarse and ISO ePM10 filter class according to ISO 16890 ensures reliable filtration even under extreme conditions, such as environments with 100% relative humidity and operating temperatures up to 100°C. Although environmental awareness was an important aspect during the development, it should be emphasized that SYNFASAN G3 can be fully incinerated, making it an environmentally sustainable option for industries striving to minimize waste. With a thickness of 15 mm, a forehead speed of 1.5 m/s and an initial pressure drop of just 30 Pa, the SYNFASAN G3 has excellent breathability and energy efficiency. It fits perfectly with our ideas. It also boasts a dust-proof capacity of 400 g on its manufacturer's data sheet, allowing for longer use without frequent replacement, reducing operating costs and improving overall system efficiency. Its ability to maintain a stable pressure drop throughout its service life and its adaptability to various environmental conditions make it the filter material of choice for industries requiring reliable and efficient air filtration solutions.

6.2. Incorporation of the filter into NIF

Incorporation of the SYNFASAN G3 filter into the NIF system involves precise cutting and preparation to ensure optimal fit and functionality.

Figure 36: Prepartion steps of an approriate size filters

Using the included device, the filter material is cut from the sheet to the desired size. At the end of this process, we use 3 guide pieces. Piece 1 cuts the initial filter block, while piece 2 divides it into three sheets of equal thickness, which are then divided into two equal parts. Piece 3 serves as a guide for cutting an octagonal pot. With dimensional markers printed on each arm of the cross (XS, S, M, L) for accurate dimensioning. Excess or broken fibers can be simply cleaned by rinsing with water, this method is made possible by the resistance of the G3 filter to water dissolution. Plans are underway to develop a new apparatus for air-based cleaning to further enhance the process. The Filter Insert Device (FID) is used to streamline the incorporation of the filter into the NEF. This involves cutting a small plastic straw to a 20 mm length, then angling one side to form a sharp tip for precise insertion. The device is disinfected with 70% alcohol to maintain sterility. Prototype testing follows to evaluate the performance of the incorporated filter, ensuring the NEF system meets its functional and protective standards effectively.

6.3. Shape fit tests and results

Shape fit tests were conducted on 40 randomly selected individuals, irrespective of sex and age, to evaluate the comfort and size compatibility of the design. Nasal measurements (A1, A2, B1, B2) according to *Figure 37* - were taken using a simple ruler, and the appropriate NIF size was determined based on a comparative chart, which has unfortunately been lost due to computer damage. Feedback indicated that the sizing chart was originally created by correlating nasal measurements with corresponding NIF sizes from the test group. Comfort levels were comparable to other nasal filters, such as Rhinix. Testers initially felt the presence of an object in the nose but soon became accustomed to it, reporting unobstructed and unnoticeable breathing during routine, non-strenuous activities when using the G3 filter. Subjective efficacy was evaluated through live tests. Testers prone to rhinorrhea wore the NIF during motorbike trips of approximately one hour to compare rhinorrhea symptoms with and without the NIF. Tests were repeated around ten times. Trips by car or bicycle were excluded due to the car's filtration system and the physiological effects of exercise, respectively. Results consistently showed that, with the NIF, nasal passages remained noticeably drier compared to non-use. The NIF also remained securely in place during sneezing. However, general consensus advises against wearing the NIF during exercise to prevent breathing obstruction; if used, light exercise requires normal nasal inhalation and oral exhalation. Notably,

filter performance declined after three hours of continuous use, emphasizing the need to replace the filter after each outing. To clean the NIF, the filter should be removed, and the shell gently washed with soap, avoiding contact with the crescent blade. After rinsing, the NIF should be disinfected with alcohol spray and stored in its container to prevent contamination.

The NIF was effective in alleviating rhinorrhea symptoms. An objective efficacy trial involved distributing NIFs to over five individuals with known airborne particle allergies. Four out of five participants reported symptom reduction, while one reported an allergic reaction likely due to inadequate glue curing during manufacturing. Allergic reactions may also occur if excess or broken fibers are not properly cleaned from the filter after cutting. Prototype testing involving 40 human volunteers of varied ages and sexes, the general shape of the XP2 Nasal Filter (NF) was well received. The XP2 model demonstrated an optimal fit within the nostrils and provided a strong, stable design. Notably, the NF remained secure even during sneezing episodes. Female participants showed a preference for the XP3 model due to its aesthetic modification capability, such as subtly raising the nose line. However, the XP3 model presented drawbacks in terms of convenience and efficiency; its specific orientation fit contrasted with the symmetrical design of the XP2, and it also had a reduced air exchange surface compared to an equally sized XP2 prototype. The 3D-printed prototypes, produced using TPU, did not induce allergic reactions in volunteers unless the crescent blade adhesive was insufficiently cured. One instance of structural failure was reported: the layer separated at the contact point between the bridge and shell under excessive force and prolonged usage, resulting in the NIF breaking. Fortunately, this incident caused no harm to the tester. Full working prototypes were distributed to eight volunteers, all with a documented history of dust allergies. Among them, five individuals provided feedback, with four reporting a noticeable reduction in allergic symptoms when using the NIF equipped with a G3 filter. The remaining three participants did not provide feedback.

In conclusion, the 3D-printed prototypes proved highly beneficial during the piloting phase, facilitating the determination of an optimized shape and serving as a proof of concept. The production process for NIF prototypes is efficient, requiring approximately one hour to print and an additional 24 hours for adhesive curing. On average, a single individual can produce five units per day using the 3D FDM printing technique.

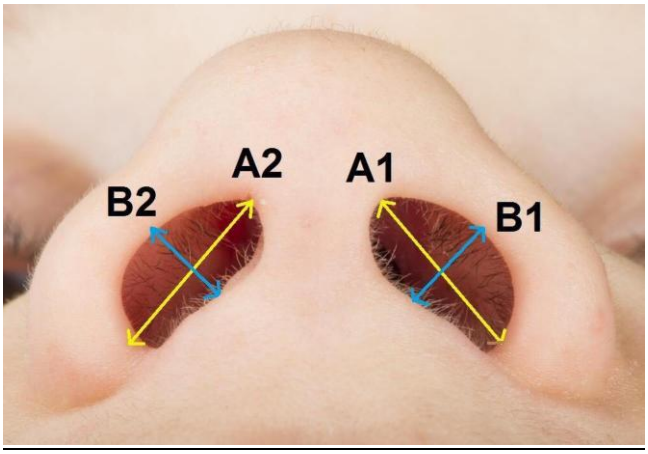

Figure 37: Measurements to be recorded for size determination

6.4. Design and prototype production of Powder Inhaler

The single-dose powder inhaler incorporates a filter designed to prevent the solid formulation from spilling when the caps are removed, while allowing unobstructed airflow during the inhalation phase. Engineered for large-scale production, each device is pre-filled with a single dose and subsequently sealed with a cap. For use, the user simply removes the cap, aligns the device with one nostril as indicated by the directional arrow, and inhales to administer the full powder content. A minor residue of particles may remain on the container's inner wall; however, this is accounted for during the initial dosing process. The device is intended for single-use only and should be discarded after use. Where possible, recycling of the container is encouraged to minimize environmental impact.

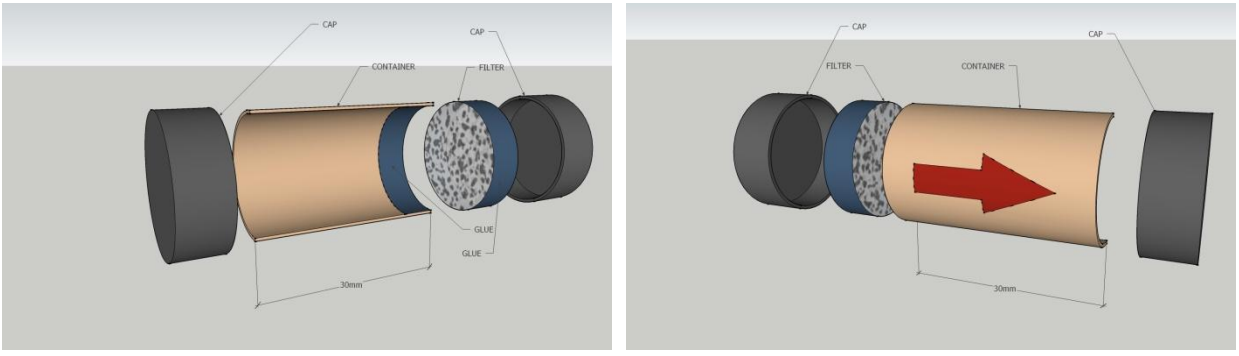

Figure 38: Powder Inhaler

7. INTEGRATION OF NASAL FILTERS WITH DRUG DELIVERY SYSTEMS

The integration of personal nasal filters with pharmaceutical nasal dispensers offers a novel solution for managing respiratory health [73]. This combination of preventive measures and targeted medication delivery provides enhanced protection, boosts the effectiveness of treatments, and may extend the lifespan of medications (Figure 4). As advancements in technology continue, ongoing research and development in this field could create new opportunities for respiratory care, ultimately improving health and quality of life for individuals globally [49]. By combining personal nose filters and pharmaceutical nasal dispensers, users can enjoy double protection. We take advantage of both systems inseparably. Nasal filters serve as the first defense, blocking the entry of allergens and pollutants into the nasal passages. In parallel, pharmaceutical nasal sprays can target existing respiratory problems and deliver drugs directly to affected areas for quick and accurate medication. In addition, nasal filters can improve the effectiveness of these pharmaceutical sprays by reducing the presence of irritants and contaminants in the nasal cavity [50]. In addition, this combination can help extend the life of the drug. Nasal filters can reduce direct contact between drug particles in the spray and nasal tissues, potentially reducing drug degradation and prolonging the shelf life and effectiveness of the drug. This benefit may also improve patients' adherence to treatment [74]. Our developments have shown that pairing nasal filters and drug dispensers with both preventive and therapeutic needs offer a comprehensive approach to respiratory care [75]. This dual approach may encourage individuals to stick to their treatment plans, improving overall compliance [76].

7.1.Solid nanoparticles for nasal formulations

Nasal drug delivery has garnered significant scientific attention for many years, following the recognition of the nasal mucosa's advantageous properties. It provides a vast surface area for quick drug absorption and serves as an alternative route to the central nervous system by bypassing the blood-brain barrier. [77]. Furthermore, it can reduce the first-pass metabolism of pharmacological agents in the liver [78]. Studies have shown that various types of active substances, including large molecules like peptides and proteins, can be effectively introduced nasally into the systemic circulation, particularly with the aid of permeability-enhancing excipients. The number of nasally administered drugs with systemic effects is growing [79]. Nasal formulations are most beneficial for diseases requiring immediate and rapid treatment. Typically, nasal preparations are solutions

or liquid-dispersed systems, such as emulsions or suspensions [80]. Although these traditional dosage forms are simple to prepare and have excellent stability, patients often report discomfort during their use, particularly liquid dripping into the pharynx, which causes an unpleasant taste. From a pharmaceutical perspective, the short duration of action and potential loss of active ingredients remains problematic. These issues can be improved by using suitable excipients with appropriate adhesive properties [81]. The objective of this research was to formulate and investigate novel solid lipid nanoparticles with enhanced active pharmaceutical ingredient (API) penetration. Alongside the API formulation, a new nasal dispenser was designed, manufactured, and tested to complement the investigation. Chlorpromazine (CPZ), an antagonist of D2 dopamine receptors and related receptors such as D3 and D5, is primarily used to treat psychotic disorders like schizophrenia and bipolar disorder [82]. Chlorpromazine was chosen for this study due to its well-characterized analytical profile and the need to reduce therapeutic doses due to frequent and serious side effects. Common side effects include movement issues, sleepiness, dry mouth, low blood pressure upon standing, and weight gain [83]. Serious side effects can include tardive dyskinesia, neuroleptic malignant syndrome, a lowered seizure threshold, and decreased white blood cell levels. In elderly patients with psychosis from dementia, chlorpromazine may increase the risk of death, and its safety during pregnancy remains uncertain [84]. Nanoparticles have revolutionized drug delivery by delivering the active compound in an unchanged, concentrated form, minimizing systemic effects and toxicity [85]. This opens new possibilities in disease diagnosis and treatment, including tumors [86]. Biodegradable nanoparticles can be produced from materials like polylactic acid (PLA), polylactic acid-glycolic acid (PLGA), and polymethyl methacrylate (PMMA) [87]. The polymer-drug conjugation enhances targeted therapy, especially with the use of penetration-enhancing amphiphilic compounds as excipients. These surface-active agents improve bioavailability for poorly soluble drugs [88]. They enhance drug permeability by modifying barriers, solubilizing micelles, fluidizing membranes, forming ion pairs, and inhibiting efflux transporters such as P-glycoprotein. However, surfactants can cause irritation, membrane damage, and cell death, so in vitro tests for cytotoxicity and irritation are necessary [89]. The combination of penetration enhancers and polymers may hold promise in improving the efficacy of active ingredients [90]. In our experiments, we applied a reliable method for producing solid nanoformulations using spray-drying technology. This method has been extensively developed in recent years to ensure high efficiency and reliability [91]. The solid-phase nanoparticles were

created using the Büchi Nano Spray Dryer B-90 HP (Büchi Labortechnik AG; Flawil, Switzerland), a specialized device designed for nanoparticle formulation at the laboratory level. The particle size distribution was assessed using a Malvern Nano Zetasizer ZSP (Malvern Panalytical; Malvern, UK), and scanning electron microscopy (SEM) was employed to analyze the morphology of the nanoparticles [79]. The size distribution of the produced particles ranged from 30 to 300 nm for various compositions. For effective nasal delivery, finely divided nano-powders require the development of specialized dosing devices. Nasal drug delivery devices were fabricated using FDM 3D printing technology, based on 3D computer designs of anatomical features, further refined with feedback from volunteers. These results can serve as a useful basis for the development of nasal drug delivery systems. The pharmaceutical industry has increasingly focused on nasal medicine in many of its developments in recent years [75]. Nasal administration has definite and well-known benefits, especially by providing direct, targeted drug delivery to the affected area, reducing systemic side effects, and improving therapeutic outcomes [82]. It allows drugs to be quickly absorbed and transported into the bloodstream, which is beneficial for drugs that require quick action [87]. However, nasal application in many therapies is challenging. These challenges, for example, include changing drug absorption due to infectious diseases or pathological anatomy causing nasal physiological changes, difficulties in penetrating the nasal epithelium, and factors affecting drug absorption in the nasal cavity [92]. To combat these problems, significant research has been devoted to nasal preparations, new drug delivery carriers, and emerging technologies [93]. Based on scientific publications on the topic, the development of submicron-sized carriers may be promising as a strategy to increase nasal drug delivery [94]. Nanoparticles, especially solid nanoparticles, play a crucial role in promoting the delivery of nasal medicines due to their ability to efficiently transport active ingredients [95]. The application of nanotechnology enables the controlled, sustained release of active ingredients, improving therapeutic efficacy [95]. The inclusion of penetrating amphiphilic compounds further improves the physical and chemical properties of preparations, enhances drug absorption and bioavailability [89]. These excipients are essential for the development of pharmaceutical products aimed at increasing the effectiveness of medicines [90]. Amphiphilic compounds with hydrophobic and hydrophilic properties may improve the solubility and stability of active substances [93]. These compounds assist in targeted delivery of active ingredients to specific tissues or cells, enhancing therapeutic effects [95]. They may also improve the controlled release of active ingredients,

allowing for prolonged therapy and simplified dosing [78]. Chlorpromazine, as a class IV drug of the Biopharmaceutical Classification System (BCS), serves as an excellent model for pharmaceutical experiments due to its low solubility and low permeability [96]. Due to its high first-pass metabolism, oral bioavailability of chlorpromazine is only 30% [97]. Thus, alternative routes of administration, such as nasal delivery, are considered. The well-known pharmacokinetic properties of chlorpromazine allow a comprehensive study of the behavior of the active substance in various preparations [98]. In this study, various formulations containing chlorpromazine and permeation enhancers were developed to improve absorption through the nasal mucosa. The use of amphiphilic compounds and solid nanoparticle formulations represents a new direction in nasal drug delivery systems. These formulations address the issues often associated with liquid formulations, such as leakage and limited bioavailability, and promise better therapeutic outcomes. This innovative approach to nasal drug delivery via finely divided powders, aided by penetration enhancers, marks significant progress in the field of nasal pharmaceutical technologies and offers new opportunities for the effective treatment of diseases.

7.2. Materials

Chlorpromazine (CPZ), Kolliphor RH 40, Kolliphor EL, Poloxamer 470, polyvinyl alcohol (PVA), Miglyol 840, hexane, glycerol, propylene glycol, and bovine serum albumin, all supplied by Sigma-Aldrich (St. Louis, MI, USA). 2-hydroxypropyl-β-cyclodextrin (HPBCD), Lauroglycol FCC, Transcutol HP, Labrafil 1944, and Labrasol were kindly provided by Gattefossé (Lyon, France). The human nasal epithelial cell line (RPMI 2650) and the human colon adenocarcinoma Caco-2 cell line were sourced from the American Type Culture Collection (ATCC, Manassas, Virginia, USA). The MTT reagent (3-(4,5-Dimethylthiazol-2-yl)-2,5-diphenyltetrazolium bromide), as well as buffer solutions such as Hank's Balanced Salt Solution (HBSS) and phosphate-buffered saline (PBS), were obtained from Sigma-Aldrich (St. Louis, MI, USA). The RPMI cell culture maintenance medium solution and TrypLE™ Express Enzyme (no phenol red) were ordered from Thermo Fisher Scientific (Waltham, MA, USA). The 96-well cell culture plates and culture flasks were acquired from VWR International (Debrecen, Hungary).

7.3. Formulation of compositions

The self-assembling emulsion systems were prepared by titrimetric dilution of the selected surfactant combination [92], incorporating 10 mg of CPZ into each formulation. The raw excipient compositions are detailed in Table 3. To check for phase separation, the mixtures were monitored over a 24-hour period.

7.4. Formulation of Solid Nano Carriers

Solid-phase nanoparticles were generated using the Büchi Nano Spray Dryer B-90 HP apparatus [99]. The SNEDDS were mixed with a 1% PVA solution and pumped into the device at a 90% pump rate. The drying gas was heated, with inlet and outlet temperatures set to 100 °C and 33 °C, respectively. During the second manufacturing stage, the inlet temperature was lowered to 60 °C, and the flow rate was adjusted from 0.11 m^3/h to 0.16 m^3/h. The product was gathered using a specialized rubber spatula. The actuator operated at 122 kHz. The physical properties of the produced systems were analyzed using two methods. The particle size distribution of the nanoparticles in their dispersed state was measured using a Malvern ZSP Nano Zetasizer (Malvern Panalytical: Malvern, UK).

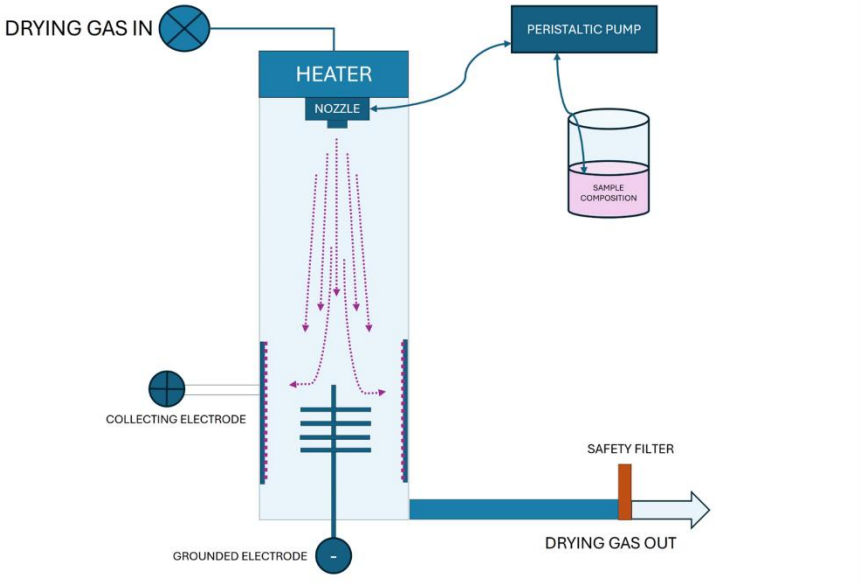

Figure 39: Schematic figure of nano spray drying technique

7.5. Scanning Electron Microscopy

The size, shape, and surface area of the formulated nanoparticles were analyzed using a Hitachi Tabletop microscope (TM3030 Plus) (Hitachi High-Technologies Corporation, Tokyo, Japan) [79]. The samples were mounted on a plate with double-sided adhesive tape, and micrographs were taken using an accelerating voltage of 5 kV.

7.6. Determination of Droplet Size

The particle size of the formulated nanoparticles was determined using a dynamic light-scattering device (Malvern ZSP Nano Zetasizer, Malvern Panalytical; Malvern, UK) [80]. A 0.5 g sample was dissolved in 100 mL of distilled water and exposed to monochromatic light. As the light interacts with the solution containing macromolecules, it scatters in all directions.

7.7. Evaluation of particle disintegration

The disintegration of nanoparticles was studied in a neutral pH physiological saline solution (0.9% sodium chloride) [77]. The disintegration time was recorded to the nearest second. Complete disintegration was verified using dynamic light scattering (DLS) analysis. Each experiment was performed with five parallel measurements. [80].

7.8. Evaluation of active ingredient dissolution

The dissolution profile of CPZ was assessed using an ERWEKA DT 950 dissolution tester. The dissolution medium consisted of artificial saline solution in compliance with the European Pharmacopoeia regulations. The active substance was quantified following the detailed protocol 2.10 using GC-MS [77]. Samples were collected at the 10th and 30th seconds after release into the medium, with subsequent samples taken every 15 seconds. Five parallel measurements were conducted during the analysis.

7.9. Stability tests

Samples were stored under controlled conditions to simulate various environmental factors affecting stability. For long-term storage, they were kept at 25°C ± 2°C with 60% ± 5% relative humidity (RH). For accelerated testing, they were stored at 40°C ± 2°C with 75% ± 5% RH, and

for refrigeration, at 5°C ± 3°C. Samples from each batch were placed in tightly sealed containers under these conditions for a 12-month period. Analytical assessments were carried out at specific intervals: initial (T0), 1 month, 3 months, 6 months, and 12 months. To evaluate any changes in particle size distribution (PSD), nanoparticles were reanalyzed using a Malvern ZSP Nano Zetasizer (Malvern Panalytical, UK) following the previously described method. Approximately 1 mg of each sample was dispersed in deionized water with gentle sonication to ensure uniformity. Measurements were made at room temperature. The experiments were carried out three times at each point in time, recording the Z-mean particle size and polydispersity index (PDI). This is because we wanted to track potential aggregation or size changes during storage. Scanning electron microscopy (SEM) was used in this experiment as well as just to investigate morphological changes in nanoparticles during formulation. The samples were mounted on aluminum stubs with guide belt and plated with gold before imaging. SEM micrographs were compared over time to detect possible changes in surface texture, shape, or aggregation that could indicate physical instability. In order to assess the stability of the drug, a gas chromatograph mass spectrometer (GC-MS) analysis with appropriate detection properties was performed in each case to quantify the active substance (API) in the nanoparticles and to identify possible degradation. A Shimadzu GCMS-QP2010 system with an SLB-5 ms capillary column (30 m x 0.25 mm inner diameter; 0.25 μm film thickness) was used for analysis. The samples were injected three times at each time point and the API concentration was determined by comparing the sample peak areas with the calibration curve derived from known standards. A decrease in API concentration of more than 5% of the initial value indicated chemical instability. The results of particle size distribution, morphology, and API content analysis were compiled and compared over time. Statistical analysis using ANOVA was performed to identify significant differences between time points and storage conditions, with a p-value of <0.05 considered statistically significant.

7.10. CPZ Content Determination

LC-MS was employed for all experiments to determine the concentration of the active ingredient. The LC-MS analysis was performed using a UHPLC system (Dionex Ultimate 3000RS) connected to a Thermo Q Exactive Orbitrap mass spectrometer (Thermo Fisher Scientific Inc., Waltham, MA, USA), featuring an electrospray ionization (ESI) source. The analysis utilized a Kinetex Polar C18 column (100 × 3 mm, 2.6 μm, 100 Å). The column temperature was maintained at 25°C. A

gradient elution was employed with solvent A (water + 0.1% formic acid) and solvent B (acetonitrile + 0.1% formic acid) at a flow rate of 0.2 mL/min. The gradient program was as follows: 0–2 min, 0% B; 2–14 min, 0–100% B; 14–15 min, 100% B; 15–16 min, 100–0% B; 16–25 min, 0% B. A 1 μL sample was injected for each analysis.

7.11. Cell Culturing

As nasal model RPMI cells were grown in appropriate medium, while colon (caco-2) cells were maintained in “DMEM” in plastic cell culture flasks, supplemented with 2 mM L-glutamine, 100 mg/L gentamycin, and 10% heat-inactivated fetal bovine serum. Cultures were kept at 37°C in a 5% CO2 incubator, with the medium being changed twice a week [100]. Cells were routinely subcultured by passaging. Prior to passaging, the flasks were coated with rat-tail collagen. For cytotoxicity assays, cells from passage numbers 10 to 30 were used [101].

7.12. MTT Viability Assay

To evaluate the toxic characteristics of the excipients selected in the study, an 3-(4,5-dimethylthiazol-2-yl)-2,5-diphenyltetrazolium bromide) assay was performed [102]. The procedure involved seeding cells in a 96-well plate at a density of 10,000 cells per well, with weekly passaging for cell maintenance. Once the cells completely covered the well surface, the experiment was initiated. The culture medium was first removed, followed by the application of the test solutions, which were incubated with the cells for 60 minutes. After this incubation, the excipients were removed, and MTT solution (5 mg/mL) was added to the wells. The cells were then incubated for an additional 3 hours. Viable cells reduced the MTT into a formazan precipitate, which was then dissolved with a 25:1 mixture of isopropanol and hydrochloric acid. The absorbance of the resulting solution was measured with a spectrophotometer, which correlates with the number of viable cells. Cell viability was expressed as a percentage relative to the PBS (negative control), and each experiment was performed in five parallel measurements.

7.13. Animals and sample collection

Labor animals used in this study received care in accordance with the national guidelines (NSMR) and the Laboratory Animals' Guide to Care and Use, as outlined by the National Academy of

Sciences and published by the National Institutes of Health (NIH Publication No. 86-23, revised 1985). The maintenance and treatment of the rats were approved by the Institutional Animal Care and Use Committee at the University of Debrecen (2/2021/DEMÁB). The animals were housed under standard conditions with a room temperature of 23 ± 2°C and a 12-hour light-dark cycle. They were provided with standard rodent chow and ad libitum tap water.

Healthy male Sprague-Dawley rats (400 ± 30 g) were anesthetized with an intraperitoneal injection of ketamine (50 mg/kg) and xylazine (10 mg/kg). The femoral vein was cannulated for blood collection. A dose of 3.0 ± 0.1 mg of CPZ preparation was administered intranasally using a Dry Powder Insufflator (Penn-Century Inc.). Blood samples were collected at baseline, and 5, 15, 30, and 60 minutes after CPZ administration. At the end of the experiments, the rats were euthanized via intravenous injection of sodium pentobarbital (200 mg/kg). The venous blood samples were allowed to coagulate at room temperature for 30 minutes to 1 hour, then centrifuged at 10,000 x g for 10 minutes. The resulting serum (non-hemolytic) was mixed with 2 volumes of acetonitrile to remove proteins. After vigorous mixing, the samples were centrifuged at 1,000 x g for 10 minutes, and the supernatant was used for GC-MS analysis [103].

7.14. Sample preparation for animal experiments

After collection, a gentle stream of N2 at 60°C were applied to dry supernatants by Turbovap LV concentrator. The samples were re-dissolved in 100 µl CH3CN and 1 µl was injected into a GC-MS equipment.

7.15. Gas chromatograph-mass spectrometric (GC-MS) analysis

The CPZ content was determined using a Shimadzu GCMS-QP2010 gas chromatograph-mass spectrometer (Kyoto, Japan) [104]. The system was configured with an SLB-5 ms capillary column (Supelco, Bellefonte, PA, USA) (30 m x 0.25 mm i.d.; 0.25 µm film thickness). Helium (He) was used as the carrier gas at a flow rate of 32 cm/sec. The temperature program for the column was as follows: initially held at 150°C for 0.25 minutes, then ramped from 150°C to 300°C at a rate of 40°C/min, and maintained at 300°C for 4 minutes. The injection port temperature was set to 280°C, while the interface temperature was 300°C. A 1 µL sample was injected into the GC-MS using a micro-syringe with a 1:50 split ratio. The mass spectrometer featured an electron ionization (EI)

source with ionization energy set to 70 eV, the ion source temperature was set to 200 °C, and the solvent cut time was 2.5 minutes. The measurements were performed in Selected Ion Monitoring (SIM) mode, with ions monitored at 318 m/z and 58 m/z, which were selected based on the SCAN mode EI spectrum.

7.16. Statistical Analysis

Data were processed and analyzed using Microsoft Excel 2013 and SigmaStat 4.0 (version 3.1; SPSS, Chicago, IL, USA, 2015), with results presented as mean ± standard deviation (SD). To compare the outcomes of the in vitro dissolution and MTT cell viability assays, one-way ANOVA and repeated-measures ANOVA were performed, followed by Tukey or Dunnett post-tests. A p-value of less than 0.05 was considered statistically significant. All experiments were conducted in quintuplicate and repeated at least five times [105].

8. RESULTS

8.1. Selection of core materials and excipients for nasal particles

In selecting excipients, we adhered to established pharmaceutical technology guidelines. The excipients chosen are of pharmaceutical grade, ensuring their purity and quality meet rigorous standards. Our decision was based on prior research and supported by international literature, ensuring careful selection of components. Potential incompatibilities between the components were assessed during formulation, and after conducting standard and accelerated stability tests, we confirmed that the systems remained stable. Notably, the formulations maintained their stability, including UV protection for the active ingredient, after 4 weeks of storage under appropriate conditions. Screening studies on in vitro cell cultures ensured that the excipients selected were non-toxic and safe. Standardized methods from the European Pharmacopoeia were employed for these investigations, and the chosen formulations were used in subsequent experiments. The formulation of the nanostructures began with developing self-assembling heterogeneous dispersed systems using CPZ and the selected excipients. A pseudoternary phase diagram was constructed to identify the range of self-organizing combinations. Nanoemulsions were created by titration, and five distinct compositions were selected, all capable of forming stable self-organizing systems. After standing for four weeks, the systems remained clear and stable. Our experiments were carried out in two phases. In the second phase, due to animal study requirements, the active ingredient concentration was increased from 100 mg to 250 mg. The compositions used in both phases are detailed in Table 3.

	Compositions	Ingredients	Quantities (mg)	Total quantity (ml)
First experimental series	Composition 1	PVA	100	50
		CPZ	100	
		Lauroglycol FCC : Kolliphor EL: Transcutol HP 1:1:1	2	
	Composition 2	PVA	100	50
		CPZ	100	
		Miglyol 840, Kolliphor EL DMSO: Glycerol 1:1:0.3:1	2	
	Composition 3	PVA	100	50
		CPZ	100	
		Labrafil 1944: Labrasol: Kolliphor EL: Propylene Glycol 1:1:1:1	2	
	Composition 4	PVA	100	50
		CPZ	100	
		Labrasol: Transcutol: Kolliphor EL: dmso:Glycerol 1:1:1:0.3:1	2	
	Composition 5	PVA	100	50
		CPZ	100	
		Lauroglycol 90: Kolliphor EL: Transcutol HP 1:1:1	2	
Second experimental series	Composition 6	PVA	100	50
		CPZ	250	
		Labrasol : Kolliphor Rh40 (2:1)	5	
	Composition 7	PVA	100	50
		CPZ	250	
		TranscutoL HP : Kolliphor Rh40 (2:1)	5	
	Composition 8	PVA	100	50
		CPZ	250	
		HPBCD	250	
	Composition 9	PVA	100	50
		CPZ	250	
		Poloxamer 407	5	

Table 3.: Formulated blends as compositions

8.2. Setting formulation parameters

The spray drying technique is commonly employed in solid nanoparticle formulations, but our experiments revealed that several manufacturing parameters were critical in achieving the desired product characteristics. During our initial attempts to prepare spray-dried nanoparticles, a significant loss of CPZ was observed. For these formulations, we set the inlet gas temperature to 100°C, which dropped to 33°C upon exiting the formulation chamber. The flow rate was set at 0.11 m³/hour, and the chamber pressure was maintained at 31 mbar. To address these issues, we implemented additional adjustments, including complete light exclusion. The inlet temperature was reduced to 60°C, and the flow rate was increased to 0.16 m³/hour, with the chamber pressure raised to 50 mbar. Despite these changes, the output temperature remained at 30°C. Other parameters, such as the feed pump rate (90% of maximum speed), nebulizer rate (80% of maximum speed), and nebulizer voltage (122 kHz), were kept constant.

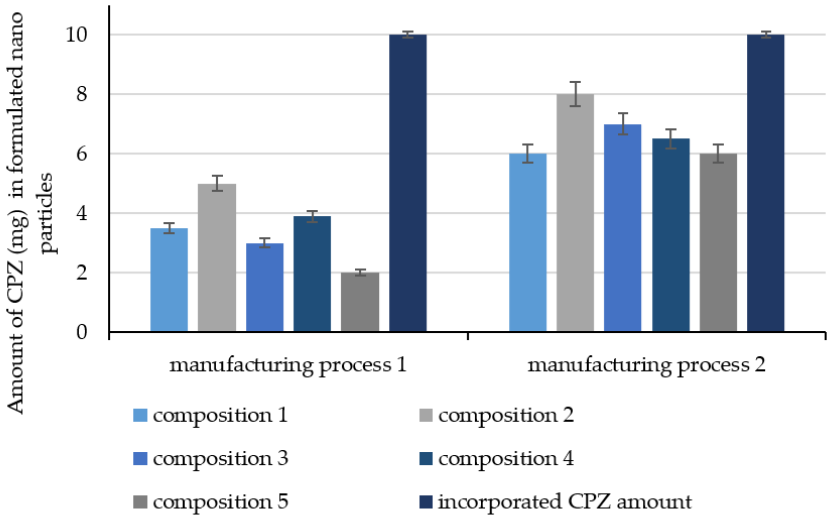

Figure 40.: Evaluated amount of CPZ (mg) in 20mg nano particles fromulated by manufcturing process 1-2. Each data point represents the mean ± SD, n = 5. In our first series of experiments, we successfully determined the settings that allow the nanospray technology to be used effectively and safely. In the second series of experiments, the samples were prepared using these parameters.

8.3. Determination of particle size and distribution

Our size and distribution studies had been demonstrated that formulations are heterogeneous dispersed systems in 10-900 nm ratio. The experiment results of the second series of measurements are summarized in Figure 41 and Figure 42

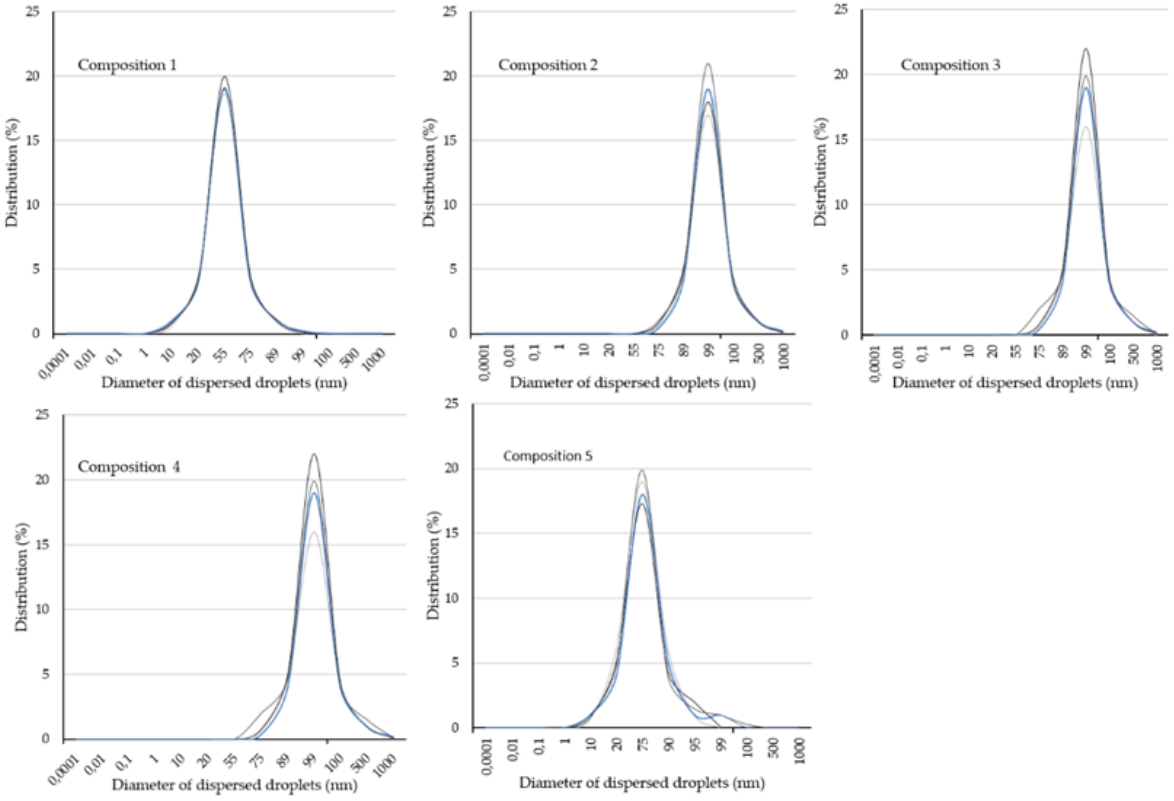

Figure 41.: Particle size distribution of composition 1-5

According to the results of the size distribution experiments, small, insignificant size differences were evaluated in parallel measurements.

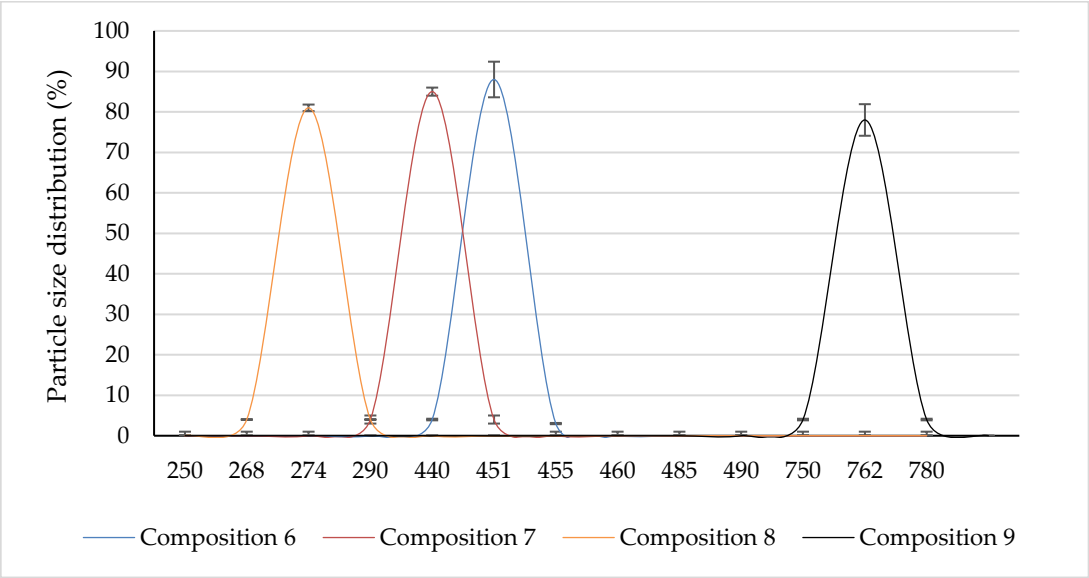

Figure 42: Particle size distribution of composition 6-9

Results of formulation procedure of composition 6 and 7 were particles with similar diameters around 450 nm. The spray drying process of composition 9 resulted in such large particles around 750 nm, while at the formulation process of composition 8 the particles found to be significantly smaller around 250 nm.

8.4. Evaluation of size and morphology of solid nanostructures

Spherical shape had been confirmed by Scanning Electron Microscope evaluations. Particle-size distribution evaluations had been demonstrated that compositions (1-5) are performing heterogeneous dispersed systems in 10-900 nm diameter ratio.

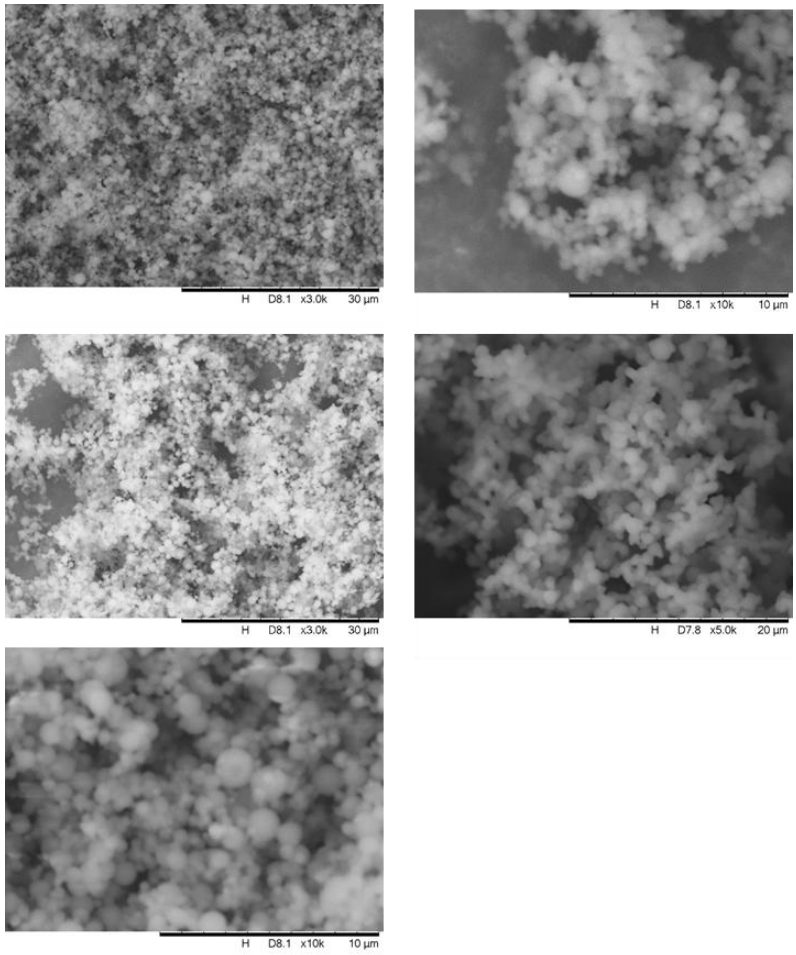

Figure 43: SEM images of solid nanoparticles (1-5). The assessment demonstrated that the compositions are performing heterogeneous dispersed systems in 10-900 nm ratio.

Scanning Electron Microscope examinations of the second experimental series, also verifyed the designed regular spherical shape. Particel-size distribution evaluations had been certified that compositions (6-9) are performing heterogeneous dispersed systems in 10-900 nm ratio.

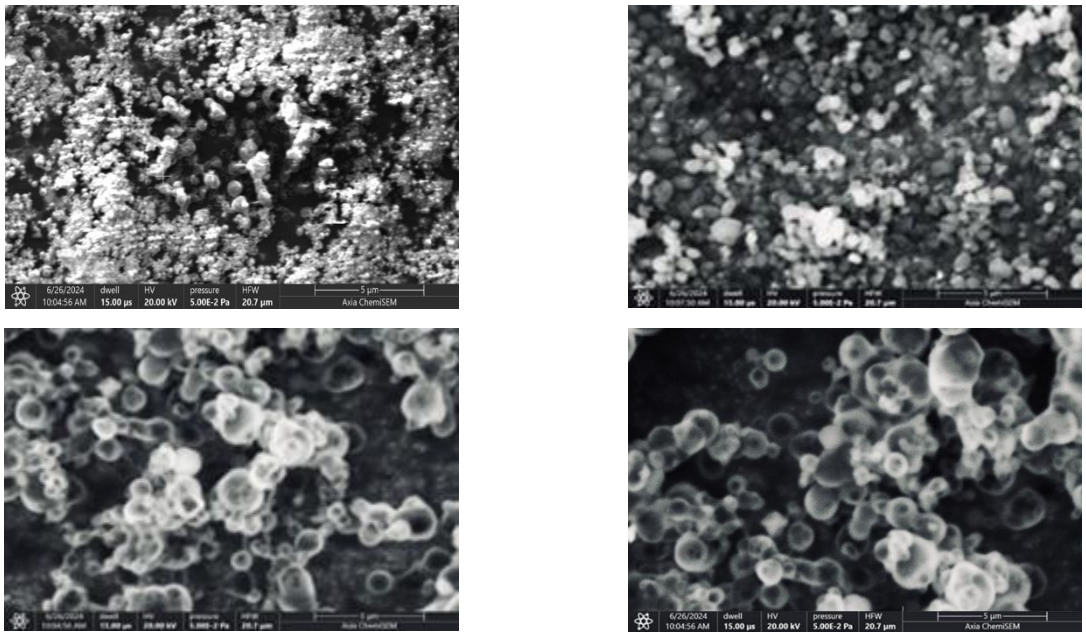

Figure 44: SEM images of solid-nanoparticles (6-9). The evaluations verified that the compositions are performing heterogeneous dispersed systems in 10-900 nm ratio.

8.5. Evaluation of the possible cytotoxic effect

The viability results from all experimental series showed that the excipients and their combinations did not cause a significant reduction in cell viability. A slight cytotoxic effect was observed at higher concentrations, which were beyond the intended application range. None of the measured values approached the IC50 threshold.

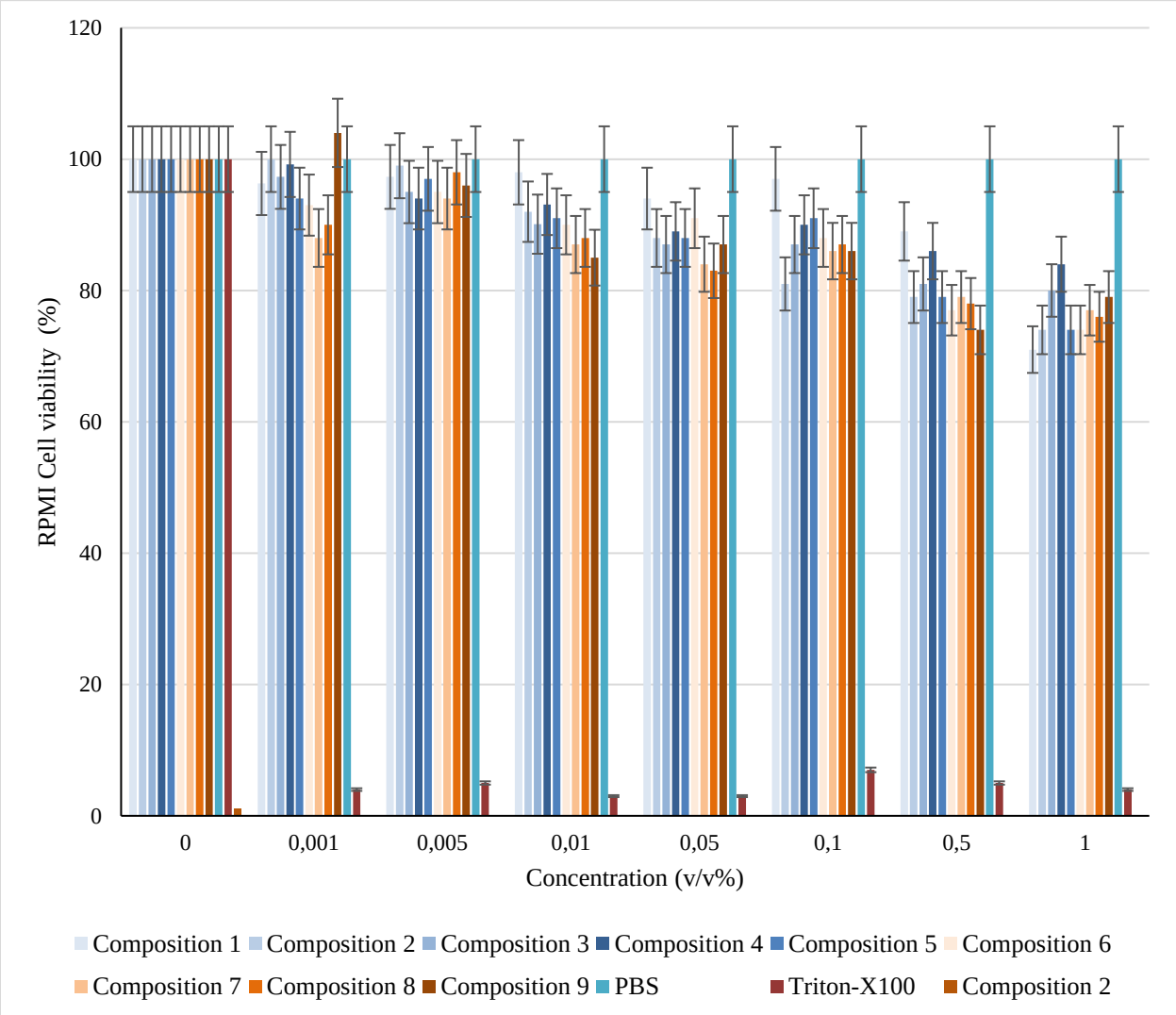

Figure 45: Effect of compositions on RPMI cell viability, evaluated by MTT cell viability assay. Each data point represents the mean ± SD, $n = 5$.

8.6. CPZ dissolution measurements

Dissolution testing revealed a rapid release of the incorporated API. Within 15 seconds, over 60% of the API was detected in each composition. The complete amount of CPZ was released after 45 seconds, and the dissolution rate remained constant after 2 minutes.

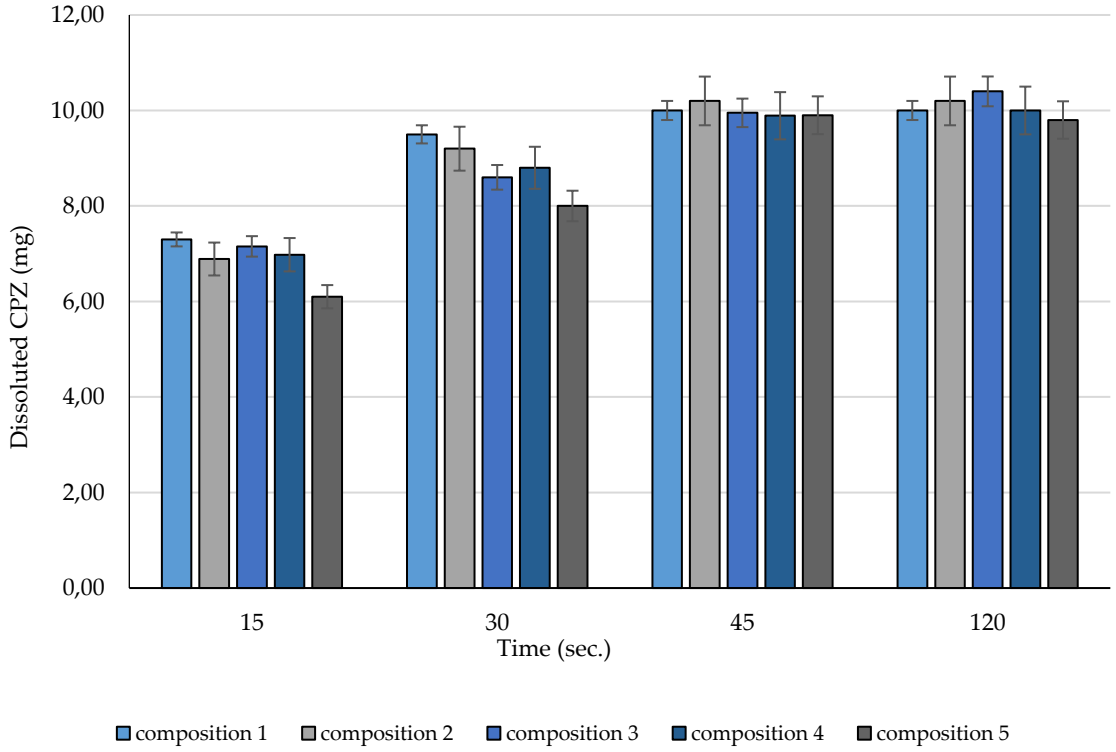

Figure 46: Amount of dissoluted CPZ after 15, 30, 45 and 120 seconds. Each data point represents the mean ± SD, $n = 5$.

In the second series of experiments PZ amount had been increased to 250 mg due to the animal experiments. The dissolution profiles of the compositions are shown in Figure 46. During the tests, an average of 75% of the incorporated active substance was detected. No significant differences were observed between the dissolution profiles across the studies.

Based on the dissolution test results, it can be concluded that approximately 70-75% of the initial 250 mg of the active ingredient was successfully encapsulated in the drug delivery systems during formulation. The variation in dissolution kinetics can be explained by the results presented in Figure 47. After analyzing the kinetic profiles, key factors for similarity and dissimilarity between the curves were assessed, revealing no significant differences in kinetics. The dissolution behavior of the systems was identified as similar.

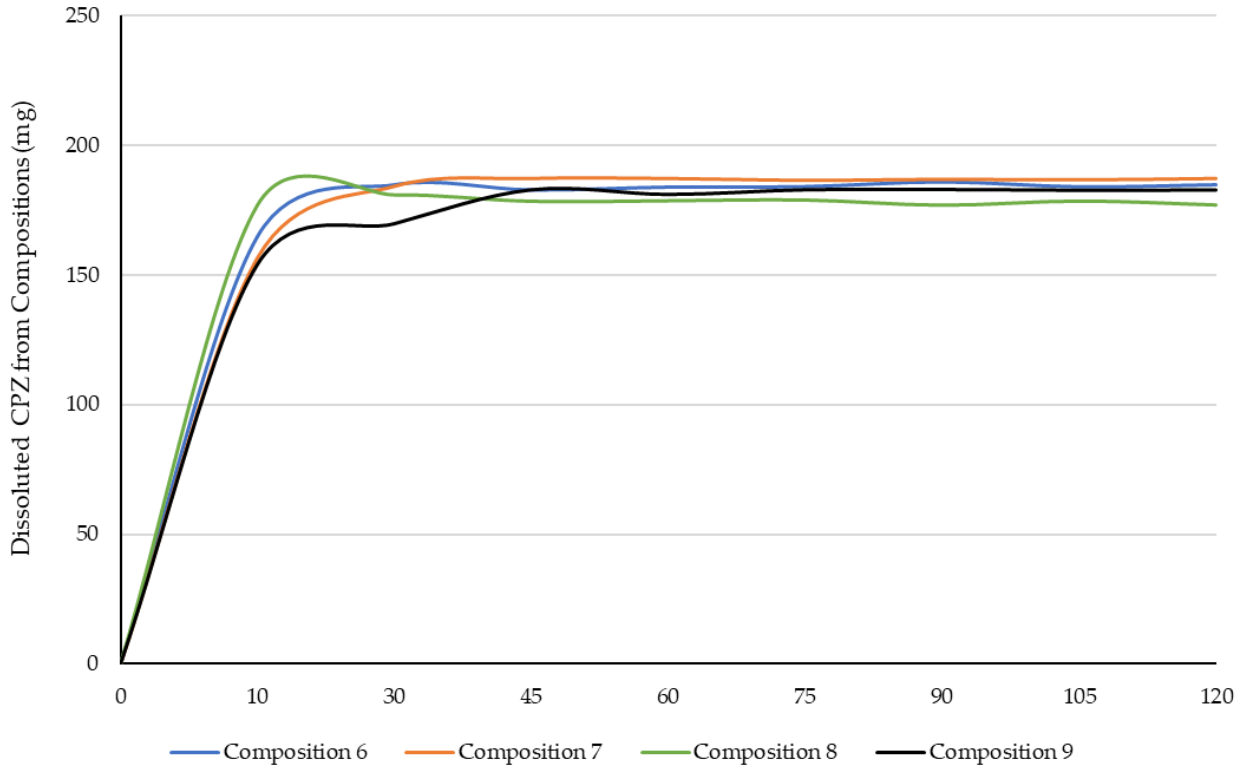

Figure 47: Dissoluted smount of CPZ (mg) from compositions

8.7. Animal studies of CPZ utilization

Before conducting the experiments, the actual CPZ content of the preparations was measured, as shown in Figure 48. The findings revealed that the CPZ content in the formulations exceeded the expected 50%. Specifically, the CPZ content for each preparation was as follows: Composition 6 – 57.7%, Composition 7 – 55.5%, Composition 8 – 56.6%, and Composition 9 – 62.9%.

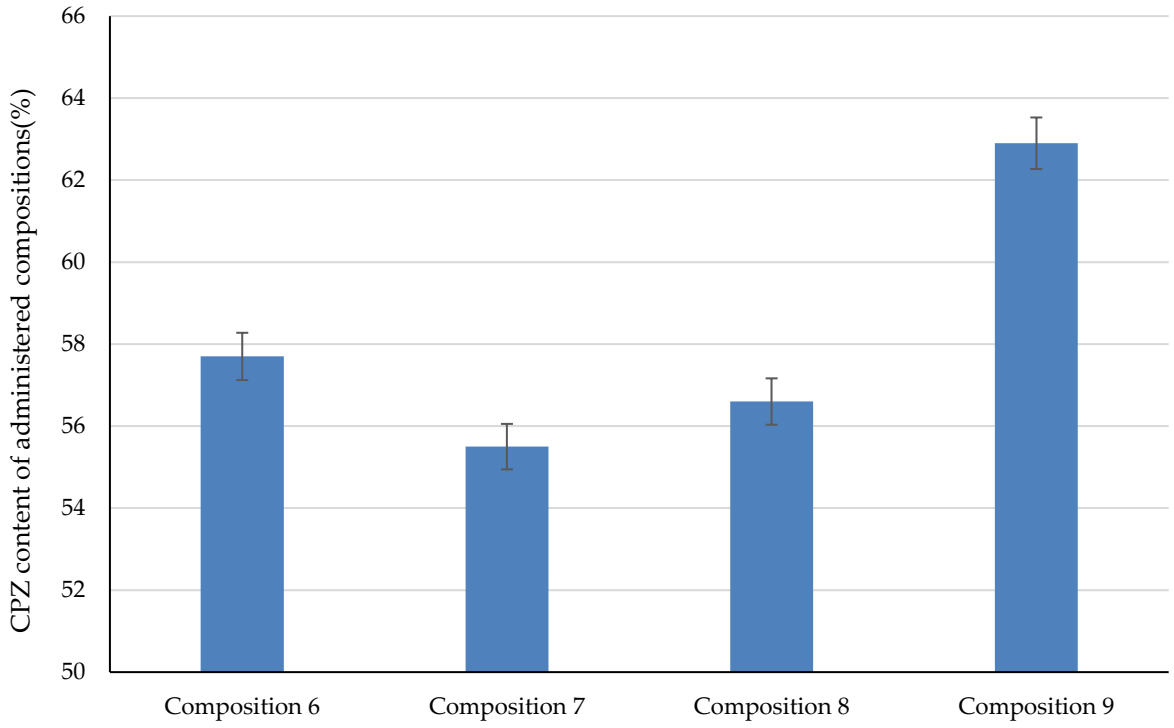

Figure 48: CPZ content of the different preparations

As shown in Figure 49, our animal experiments indicated that Compositions 8 and 9 were the most promising for further development. After administering Composition 9, the blood concentration of CPZ increased rapidly, reaching its peak quickly, followed by a significant decrease in drug levels. For Composition 8, the measured blood levels were also considerably higher than those observed with Compositions 6 and 7. Furthermore, Composition 8 displayed a rapid rise in blood levels, followed by a notable plateau phase, which could present additional benefits.

Several factors could explain this phenomenon related to nanoparticles containing CD excipients. HPBCD is recognized for its ability to form inclusion complexes with drugs, which can substantially improve their solubility and bioavailability.

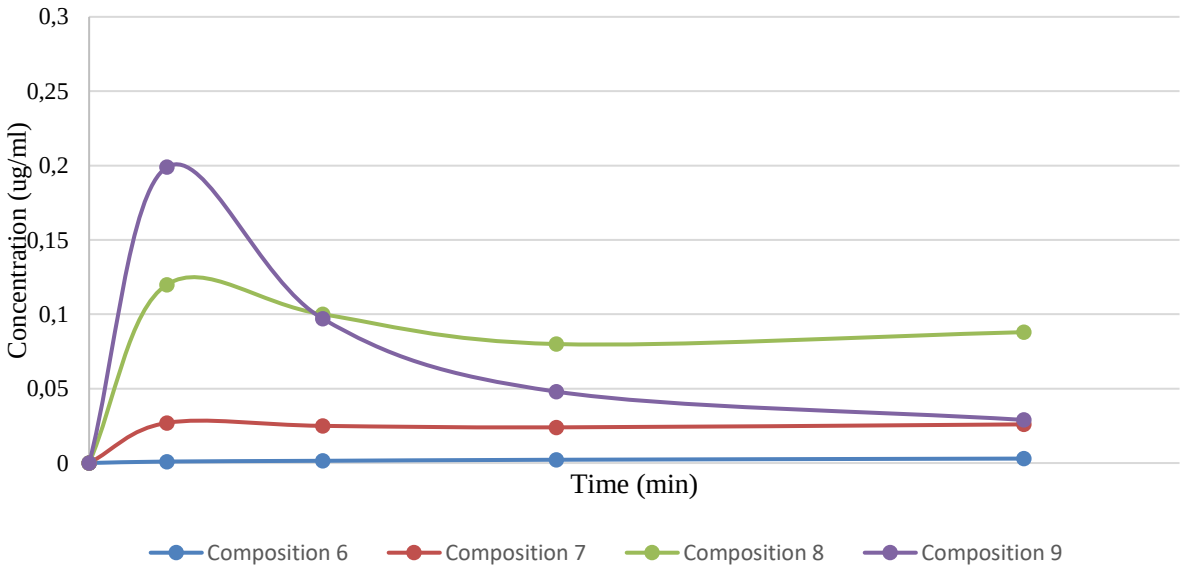

Figure 49: blood CPZ concentration of the different preparations

Following disintegration, the HPBCD-drug complex dissolves easily, promoting faster absorption across biological membranes. Based on our experiments, we concluded that the rapid degradation of nanoparticles containing HPBCD is likely to contribute to the rapid release of the drug in a more absorbable form. This can lead to a faster appearance and prolonged concentration in the blood. This is presumably due to effective initial absorption. In addition, cyclodextrins, as confirmed by our previous experiments in the department, can improve the permeability of the drug through mucous membranes, increasing the initial absorption rate and maintaining prolonged drug levels in circulation. In addition, as literature data, HPBCD can protect the drug from degradation, ensuring a more stable release and absorption profile over time. Based on our experimental results, the combination of increased solubility, efficient absorption, and improved membrane penetration attributed to HPBCD likely explains the elongated blood levels observed in our animal studies despite the rapid disintegration of nanoparticles. This insight is valuable, and we plan to investigate this phenomenon further in our future research.

9. DISCUSSION

The first part of my dissertation, summarizing my experimental results, highlights the potential of personalized nasal filters to revolutionize healthcare through targeted applications of respiratory protection and drug delivery. It is clearly proven that customized nasal filters can help protect against airborne pathogen agents. The small devices I developed are small devices placed in the nasal passage, easy-to-use 3D printed equipment that filters out harmful particles and allergens. These filters can improve microambient air quality and can be tailored to individual needs, providing effective protection for people suffering from allergies, asthma and other respiratory diseases. When combined with an appropriate delivery system, filters offer a new approach to drug delivery, taking advantage of the high absorption capacity of the nasal mucosa and the well-known tendency to deliver drugs more efficiently and with fewer side effects. The studies underlying my dissertation emphasize the importance of multidisciplinary collaboration between engineers and healthcare professionals in the development and clinical evaluation of these filters. Promising future developments I have reviewed in my work include incorporating ultrafine and active filter technologies, using sustainable and recyclable materials, and integrating IoT to track filter performance. All these can contribute to the success of the results of the thematic area. Personalized nasal filters represent a significant step forward in both patient care and drug delivery, as they have the potential to improve patients' quality of life. However, it is important to stress that continuous research and development is essential for the widespread adoption of these innovative tools in healthcare and among ordinary users. Formulation studies focused on the design of solid-phase nano drug delivery systems for nasal application using amphiphilic excipients. The study that underpinned my dissertation identified key manufacturing parameters of nanospray drying, such as temperature and light exclusion, which significantly improved the stability of active pharmaceutical ingredients (APIs). In our experiment, five different self-organizing, heterogeneous dispersed systems were produced, demonstrating the potential of nano spray drying technology to create stable and efficient drug carriers. Safe applicability is the basis of all pharmaceutical technology developments. Therefore, all formulations were subjected to in vitro cell culture diocompatibility tests. Biocompatibility tests on RPMI 2650 nasal cells confirmed the safety of the excipients used, while physical tests using instrumental analytical methods showed that the systems meet size and morphological standards. Stability and dissolution tests showed rapid API release and stable formulation, which was further confirmed by microCT analysis, which

ruled out excessive nanoparticle aggregation. A 3D-printed nasal dosing device ensured precise administration, making the system suitable for practical use. These findings provide a foundation for future development of nasal or oral nanosystems and related biocompatibility tests, contributing to the advancement of targeted drug delivery systems. To complete the phenomenon we investigated various nasal formulations containing chlorpromazine and amphiphilic permeation enhancers to improve drug absorption through the nasal mucosa. Amphiphilic compounds were shown to stabilize particle size, contributing to consistent therapeutic outcomes. Among the tested compositions, Composition 8 (formerly Composition 3) exhibited the least impact on cell viability, indicating its safety, while Composition 5 (formerly Composition 4), containing Poloxamer 407, showed lower tolerability due to its cytotoxic potential. Dissolution studies revealed no significant differences among the compositions, though Composition 8 ensured the fastest disintegration. Animal studies demonstrated that Composition 8 was the most biocompatible, while Composition 5, despite its promising results, required cautious use due to potential nasal mucosa irritation. Based on our experimental results, we showed that amphiphilic compounds play a key role in enhancing drug absorption and stability. This can also make a major contribution to the work of other working groups. Based on our results, we see that future research should focus on optimizing the concentration of excipients and exploring new amphiphilic compounds in order to develop innovative nasal medicines. These results provide a valuable basis for the creation of future pilot products and the development of nasal pharmaceutical technologies. The research conducted in the three studies underpinning my dissertation examined in detail the transformative potential of nasal drug delivery and respiratory protection systems in modern medicine. The development of customised nasal filters highlights innovative approaches to improving air quality and enabling accurate, targeted drug delivery. By adapting these filters to individual needs, patients with respiratory diseases such as asthma and allergies can experience increased protection and a better quality of life. In addition, rapid drug absorption through the nasal mucosa offers a promising alternative to systemic drug administration, minimizing side effects and improving therapeutic outcomes. In the second phase of my experimental work, we focused on solid-phase nano drug carriers. We have proven the versatility and efficiency of nanospray drying technology in pharmaceutical applications in combination with nasal application. The ability to create stable, biocompatible nanoparticle formulations paves the way for efficient drug delivery systems that are key to treating a variety of conditions. The study's findings on manufacturing

parameters and biocompatibility tests provide basic guidance for future formulations and highlight the importance of interdisciplinary collaboration in the development of innovative medical devices. The study in the third phase of my experimental work emphasizes the critical role of amphiphilic compounds in improving drug stability, absorption, and safety. We pointed out that identifying optimal formulations, such as Composition 8, provides valuable insights to create effective and well-tolerated nasal drug delivery systems. The results also underline the importance of balancing efficacy and safety, especially for preparations containing excipients such as Poloxamer 407. This experimental work I hope could contribute to the delivery of nasal medicines and respiratory protection. My experimental results can provide practical solutions and lay the foundation for future innovations in this field. Pharmaceutical developments require extraordinary resources, financial and skill requirements. During my work, I tried to get to know the topic thoroughly and to create and analyze a research direction that can really contribute to the innovation of nasal drug development and the development of the therapeutic field.

10. SUMMARY

During my research, I developed and investigated a drug delivery method that can be connected with nasal protective devices, representing a drug therapy option. In the first experiments of the research, I investigated the development of personalized nasal filters and the application of solid-phase nano drug carriers, emphasizing their importance in modern medicine. In my research, I have proven that individualized nasal filters can provide effective protection while improving the quality of the air we breathe and creating opportunities for targeted drug delivery. The customizable design of the 3D-printed compact filters developed by me allows people suffering from allergies, asthma and other respiratory diseases to effectively protect themselves. The other main pillar of my research work was the development of nanotechnology drug carriers, during which we proved the applicability of nanospray drying to create stable and effective drug formulations. During the studies, five different, self-organizing, heterogeneous dispersion systems were produced, which prove the versatility of the technology of nanospray drying. Key manufacturing parameters, such as temperature and light exclusion, had a significant impact on the stability of active pharmaceutical ingredients. Physical and biological tests have confirmed that the nanoparticles produced in this way meet size and morphological requirements, while their stability and rapid release of active substances allow them to function as effective drug carriers. Biocompatibility tests performed on RPMI 2650 nasopharyngeal cells confirmed the safe use of formulations, while dissolution experiments showed rapid release and stable formulations. Examining the role of various amphiphilic excipients, the results revealed that certain formulations, such as Composition 8, have high biocompatibility and rapid dispersibility, while others, such as formulas containing Poloxamer 407, require cautious use due to their potential cytotoxic effects.

The results of the research may not only lead to breakthroughs in the development of nasal filters and nano drug carriers, but may also contribute to the development of targeted drug delivery systems. In future research, it is worth further optimizing excipient concentrations and further developing the efficacy and stability of drugs that can be administered through the nasal mucosa by including new amphiphilic compounds. The results may provide a basis for the development of pilot products and the further promotion of nasal pharmaceutical technology innovations.

11. REFERENCES

1. Hanson, L.R.; Frey, W.H. Intranasal Delivery Bypasses the Blood-Brain Barrier to Target Therapeutic Agents to the Central Nervous System and Treat Neurodegenerative Disease. BMC Neurosci 2008,9, S5.

2. Eleni, K.; Paraskevi, P.; Georgia, V. Advances in intranasal vaccine delivery: A promising non-invasive route of immunization. Vaccine, 2023;18.235.

3. Ozsoy, Y.; Gungor, S.; Cevher, E. Nasal Delivery of High Molecular Weight Drugs. Molecules 2009,14, 3754–3779.

4. Pires, P.C.; Rodrigues, M.; Alves, G.; Santos, A.O. Strategies to Improve Drug Strength in Nasal Preparations for Brain Delivery of Low Aqueous Solubility Drugs. Pharmaceutics 2022, 14, 588.

5. Wong, I.Y.Z.; Soh, S.E.; Chng, S.Y.; Shek, L.P.-C.; Goh, D.Y.T.; Van Bever, H.P.S.; Lee, B.W. Compliance with Topical Nasal Medication—An Evaluation in Children with Rhinitis. Pediatr. Allergy Immunol. 2010, 21, 1146–1150.

6. Musumeci, T.; Bonaccorso, A.; Puglisi, G. Epilepsy Disease and Nose-to-Brain Delivery of Polymeric Nanoparticles: An Overview. Pharmaceutics 2019, 11, 118.

7. Harrold, M.W.; Chang, Y.A.; Wallace, R.A.; Farooqui, T.; Wallace, L.J.; Uretsky, N.; Miller, D.D. Charged Analogs of Chlorpromazine as Dopamine Antagonists. J. Med. Chem . 1987, 30, 1631–1635.

8. Li, L.; Liu, X.; Cui, Y.; Chen, Y.; Wu, H.; Wang, J.; Gong, X.; Gao, X.; Yang, L.; Li, J.; et al. Novel chlorpromazine derivatives as anti-endometrial carcinoma agents with reduced extrapyramidal side effects. Bioorganic Chem. 2022, 127, 106008.

9. Mackay, E.V. Progressive chlorpromazine jaundice during pregnancy. Med. J. Aust. 1960, 1, 209–212.

10. Najahi-Missaoui, W.; Arnold, R.D.; Cummings, B.S. Safe Nanoparticles: Are We There Yet? Int. J. Mol. Sci. 2020, 22, 385.

11. Hoffmann, C.; Shen, C.; Le Tourneau, C. Nanoparticle Therapy for Head and Neck Cancers. Curr. Opin. Oncol. 2022, 34, 177–184.

12. Kallinteri, P.; Higgins, S.; Hutcheon, G.A.; St. Pourçain, C.B.; Garnett, M.C. Novel Functionalized Biodegradable Polymers for Nanoparticle Drug Delivery Systems. Biomacromolecules 2005, 6, 1885–1894.

13. LESLIE, R. Surface-Active Agents. Manuf. Chem. Aerosol News 1947, 18, 149–150.

14. Rundle, C.W.; Presley, C.L.; Militello, M.; Barber, C.; Powell, D.L.; Jacob, S.E.; Atwater, A.R.; Watsky, K.L.; Yu, J.; Dunnick, C.A. Hand Hygiene during COVID-19: Recommendations from the American Contact Dermatitis Society. J. Am. Acad. Dermatol. 2020, 83, 1730–1737

15. Alshweiat, A.; Ambrus, R.; Csóka, I. Intranasal Nanoparticulate Systems as Alternative Route of Drug Delivery. Curr. Med. Chem. 2019, 26, 6459–6492.

16. Sibinovska, N.; Žakelj, S.; Trontelj, J.; Kristan, K. Applicability of RPMI 2650 and Calu-3 Cell Models for Evaluation of Nasal Formulations. Pharmaceutics 2022, 14, 369.

17. Mazayen, Z.M.; Ghoneim, A.M.; Elbatanony, R.S.; Basalious, E.B.; Bendas, E.R. Pharmaceutical Nanotechnology: From the Bench to the Market. Futur. J. Pharm. Sci. 2022, 8, 12.

18. Strojewski, D.; Krupa, A. Spray Drying and Nano Spray Drying as Manufacturing Methods of Drug-Loaded Polymeric Particles. Polym. Med. 2022, 52, 101–111.

19. Harsha, S.; E Aldhubiab, B.; Nair, A.; Abdulrahman Alhaider, I.; Attimarad, M.; Narayanaswamay, V.; Srinivasan, V.; Gangadhara, N.; Asif, A. Nanoparticle formulation by Büchi B-90 Nano Spray Dryer for oral mucoadhesion. Drug Des. Devel. Ther. 2015, 9, 273–282.

20. Abd-Rabou, A.A.; Ahmed, H.H.; Shalby, A.B. Selenium Overcomes Doxorubicin Resistance in Their Nano-Platforms Against Breast and Colon Cancers. Biol. Trace Elem. Res. 2020, 193, 377–389.

21. Fischer, E.R.; Hansen, B.T.; Nair, V.; Hoyt, F.H.; Dorward, D.W. Scanning Electron Microscopy. Curr. Protoc. Microbiol. 2012, 25, 2B.2.1–2B.2.47.

22. Ferreyro B.L., Angriman F., Munshi L., Del Sorbo L., Ferguson N.D., Rochwerg B., Ryu M.J., Saskin R., Wunsch H., da Costa B.R., et al. Association of Noninvasive Oxygenation Strategies with All-Cause Mortality in Adults with Acute Hypoxemic Respiratory Failure. JAMA. 2020;324:57. doi: 10.1001/jama.2020.9524. -

23. Freiberg A., Horvath K., Hahne T.M., Drössler S., Kämpf D., Spura A., Buhs B., Reibling N., De Bock F., Apfelbacher C., et al. Beeinflussung Der Psychosozialen Entwicklung von Kindern Und Jugendlichen Durch Das Tragen von Gesichtsmasken Im Öffentlichen Raum Zur Prävention von Infektionskrankheiten: Ein Systematischer Review. Bundesgesundheitsblatt Gesundheitsforschung Gesundheitsschutz. 2021;64:1592–1602. doi: 10.1007/s00103-021-03443-5. -

24. Magalhães P.A.F., D'Amorim A.C.G., de Oliveira E.F.A.L., Ramos M.E.A., Mendes A.P.D.d.A., Barbosa J.F.d.S., Reinaux C.M.A. Alternância de Máscara Nasal Com Pronga Nasal Reduz a Incidência de Lesão Nasal Moderada a Grave Em Prematuros Em Uso de Ventilação Não Invasiva. Rev. Bras. Ter. Intensiv. 2022;34:247–254. doi: 10.5935/0103-507X.20220022-pt. -

25. Olin A.C., Hellgren J., Karlsson G., Ljungkvist G., Nolkrantz K., Torén K. Nasal Nitric Oxide and Its Relationship to Nasal Symptoms, Smoking and Nasal Nitrate. Rhinology. 1998;36:117–121.

26. Farneti P., Sorace F., Tasca I. Personal Protective Equipment for ENT Activity during COVID-19 Pandemic. Eur. Arch. Oto-Rhino-Laryngol. 2020;277:2933–2935. doi: 10.1007/s00405-020-06177-3.

27. Kesavan S., Amirav I. Is Aerosol Delivery by High-flow Nasal Cannula in Children an Effective Alternative to Face Mask Aerosol Nebulization? Pediatr. Pulmonol. 2019;54:1873–1874. doi: 10.1002/ppul.24480.

28. Hasegawa M., Kern E.B. The Human Nasal Cycle. Mayo Clin. Proc. 1977;52:28–34. doi: 10.1097/00006534-197708000-00039.

29. Maniaci A., Ferlito S., Bubbico L., Ledda C., Rapisarda V., Iannella G., La Mantia I., Grillo C., Vicini C., Privitera E., et al. Comfort Rules for Face Masks among Healthcare Workers during COVID-19 Spread. Ann. Ig. 2021;33:615–627. doi: 10.7416/ai.2021.2439.

30. Mauritzson-Sandberg E. Psychological Effects on Prolonged Use of Respiratory Protective Devices in Children. Ergonomics. 1991;34:313–319. doi: 10.1080/00140139108967315.

31. Grigatti A., Gefen A. The Biomechanical Efficacy of a Hydrogel-based Dressing in Preventing Facial Medical Device-related Pressure Ulcers. Int. Wound J. 2022;19:1051–1063. doi: 10.1111/iwj.13701.

32. Ferraz L.C.C., Guedes B.L.d.S., Lúcio I.M.L., Santos R.C.S. Desenvolvimento de Protetor Nasal Anatômico Para Recém-Nascidos Em Uso de Pronga. Rev. Esc. Enferm. USP. 2020;54:e03618. doi: 10.1590/s1980-220x2019005603618.

33. Scarano A., Inchingolo F., Rapone B., Festa F., Rexhep Tari S., Lorusso F. Protective Face Masks: Effect on the Oxygenation and Heart Rate Status of Oral Surgeons during Surgery. Int. J. Environ. Res. Public Health. 2021;18:2363. doi: 10.3390/ijerph18052363.

34. Yamasaki T., Komasawa N., Kido H., Minami T. Contribution of the Nasal Passage to Face Mask Ventilation: A Prospective Blinded Randomized Crossover Trial. Can. J. Anaesth. 2017;64:935–939. doi: 10.1007/s12630-017-0911-3.

35. Kayser V., Ramzan I. Vaccines and Vaccination: History and Emerging Issues. Hum. Vaccines Immunother. 2021;17:5255–5268. doi: 10.1080/21645515.2021.1977057.

36. Peters R., Ee N., Peters J., Booth A., Mudway I., Anstey K.J. Air Pollution and Dementia: A Systematic Review. J. Alzheimer's Dis. 2019;70:S145–S163. doi: 10.3233/JAD-180631.

37. Shah A.S., Langrish J.P., Nair H., McAllister D.A., Hunter A.L., Donaldson K., Newby D.E., Mills N.L. Global Association of Air Pollution and Heart Failure: A Systematic Review and Meta-Analysis. Lancet. 2013;382:1039–1048. doi: 10.1016/S0140-6736(13)60898-3.

38. Tran H.M., Chen T.-T., Lu Y.-H., Tsai F.-J., Chen K.-Y., Ho S.-C., Wu C.-D., Wu S.-M., Lee Y.-L., Chung K.F., et al. Climate-Mediated Air Pollution Associated with COPD Severity. Sci. Total Environ. 2022;843:156969. doi: 10.1016/j.scitotenv.2022.156969.

39. Sousa A.C., Pastorinho M.R., Masjedi M.R., Urrutia-Pereira M., Arrais M., Nunes E., To T., Ferreira A.J., Robalo-Cordeiro C., Borrego C., et al. Issue 1—"Update on Adverse Respiratory Effects of Outdoor Air Pollution" Part 2): Outdoor Air Pollution and Respiratory Diseases: Perspectives from Angola, Brazil, Canada, Iran, Mozambique and Portugal. Pulmonology. 2022;28:376–395. doi: 10.1016/j.pulmoe.2021.12.007.

40. Jia Y., Lin Z., He Z., Li C., Zhang Y., Wang J., Liu F., Li J., Huang K., Cao J., et al. Effect of Air Pollution on Heart Failure: Systematic Review and Meta-Analysis. Environ. Health Perspect. 2023;131:76001. doi: 10.1289/EHP11506.

41. Bhadauria S., Dixit A., Singh D. Estimation of Air Pollution Tolerance and Anticipated Performance Index of Roadside Plants along the National Highway in a Tropical Urban City. Environ. Monit. Assess. 2022;194:808. doi: 10.1007/s10661-022-10483-0.

42. Gajski G., Gerić M., Pehnec G., Matković K., Rinkovec J., Jakovljević I., Godec R., Žužul S., Bešlić I., Cvitković A., et al. Associating Air Pollution with Cytokinesis-Block Micronucleus Assay Parameters in Lymphocytes of the General Population in Zagreb (Croatia) Int. J. Mol. Sci. 2022;23:83. doi: 10.3390/ijms231710083.

43. Zhang X., Xia Q., Lai Y., Wu B., Tian W., Miao W., Feng X., Xin L., Miao J., Wang N., et al. Spatial Effects of Air Pollution on the Economic Burden of Disease: Implications of Health and Environment Crisis in a Post-COVID-19 World. Int. J. Equity Health. 2022;21:161. doi: 10.1186/s12939-022-01774-6. .

44. Liu C., Cai J., Chen R., Sera F., Guo Y., Tong S., Li S., Lavigne E., Correa P.M., Ortega N.V., et al. Coarse Particulate Air Pollution and Daily Mortality: A Global Study in 205 Cities. Am. J. Respir. Crit. Care Med. 2022;206:999–1007. doi: 10.1164/rccm.202111-2657OC.

45. Ren X., Huang S., Wang J., Xu X. The Impact of Urbanization on Air Quality in Africa from Time and Spatial Perspectives. Environ. Sci. Pollut. Res. Int. 2022;29:74699–74714. doi: 10.1007/s11356-022-21109-w.

46. Landry S.A., Subedi D., Barr J.J., MacDonald M.I., Dix S., Kutey D.M., Mansfield D., Hamilton G.S., Edwards B.A., Joosten S.A. Fit-Tested N95 Masks Combined With Portable High-Efficiency Particulate Air Filtration Can Protect Against High Aerosolized Viral Loads Over Prolonged Periods at Close Range. J. Infect. Dis. 2022;226:199–207. doi: 10.1093/infdis/jiac195.

47. Seibt R., Bär M., Rieger M.A., Steinhilber B. Limitations in Evaluating COVID-19 Protective Face Masks Using Open Circuit Spirometry Systems: Respiratory Measurement Mask Introduces Bias in Breathing Pressure and Perceived Respiratory Effort. Physiol. Meas. 2023;44:015001. doi: 10.1088/1361-6579/aca7ab.

48. Mahmoudi A., Tavakoly Sany S.B., Ahari Salmasi M., Bakhshi A., Bustan A., heydari S., Rezayi M., Gheybi F. Application of Nanotechnology in Air Purifiers as a Viable Approach to Protect against Corona Virus. IET Nanobiotechnol. 2023;17:289–301. doi: 10.1049/nbt2.12132.

49. Rogak S.N., Rysanek A., Lee J.M., Dhulipala S.V., Zimmerman N., Wright M., Weimer M. The Effect of Air Purifiers and Curtains on Aerosol Dispersion and Removal in Multi-Patient Hospital Rooms. Indoor Air. 2022;32:e13110. doi: 10.1111/ina.13110.

50. Khan M.T., Shah I.A., Hossain M.F., Akther N., Zhou Y., Khan M.S., Al-Shaeli M., Bacha M.S., Ihsanullah I. Personal Protective Equipment (PPE) Disposal during COVID-19: An Emerging Source of Microplastic and Microfiber Pollution in the Environment. Sci. Total Environ. 2023;860:160322. doi: 10.1016/j.scitotenv.2022.160322.

51. Hasan M., Islam A.R.M.T., Jion M.M.M.F., Rahman M.N., Peu S.D., Das A., Bari A.B.M.M., Islam M.S., Pal S.C., Islam A., et al. Personal Protective Equipment-Derived Pollution during Covid-19 Era: A Critical Review of Ecotoxicology Impacts, Intervention Strategies, and Future Challenges. Sci. Total Environ. 2023;887:164164. doi: 10.1016/j.scitotenv.2023.164164.

52. Chen R., Zhang X., Wang P., Xie K., Jian J., Zhang Y., Zhang J., Yuan Y., Na P., Yi M., et al. Transparent thermoplastic polyurethane air filters for efficient electrostatic capture of particulate matter pollutants. Nanotechnology. 2019;30:015703. doi: 10.1088/1361-6528/aae611.

53. Liang H., Ji Y., Ge W., Wu J., Song N., Yin Z., Chai C. Release kinetics of microplastics from disposable face masks into the aqueous environment. Sci. Total Environ. 2022;816:151650. doi: 10.1016/j.scitotenv.2021.151650.

54. Moghadasi H., Mollah M.T., Marla D., Saffari H., Spangenberg J. Computational Fluid Dynamics Modeling of Top-Down Digital Light Processing Additive Manufacturing. Polymers. 2023;15:2459. doi: 10.3390/polym15112459.

55. Jiang J., Du C., Hu Y., Yuan H., Wang J., Pan Y., Bao L., Dong L., Li C., Sun Y., et al. Diagnostic Performance of Computational Fluid Dynamics (CFD)-Based Fractional Flow Reserve (FFR) Derived from Coronary Computed Tomographic Angiography (CCTA) for Assessing Functional Severity of Coronary Lesions. Quant. Imaging Med. Surg. 2023;13:1672–1685. doi: 10.21037/qims-22-521.

56. Quodbach J., Bogdahn M., Breitkreutz J., Chamberlain R., Eggenreich K., Elia A.G., Gottschalk N., Gunkel-Grabole G., Hoffmann L., Kapote D., et al. Quality of FDM 3D Printed Medicines for Pediatrics: Considerations for Formulation Development, Filament Extrusion, Printing Process and Printer Design. Ther. Innov. Regul. Sci. 2022;56:910–928. doi: 10.1007/s43441-021-00354-0.

57. Serrano D.R., Kara A., Yuste I., Luciano F.C., Ongoren B., Anaya B.J., Molina G., Diez L., Ramirez B.I., Ramirez I.O., et al. 3D Printing Technologies in Personalized Medicine, Nanomedicines, and Biopharmaceuticals. Pharmaceutics. 2023;15:313. doi: 10.3390/pharmaceutics15020313.

58. Ahmad J., Garg A., Mustafa G., Mohammed A.A., Ahmad M.Z. 3D Printing Technology as a Promising Tool to Design Nanomedicine-Based Solid Dosage Forms: Contemporary Research and Future Scope. Pharmaceutics. 2023;15:1448. doi: 10.3390/pharmaceutics15051448.

59. Abourehab M.A.S., Pramanik S., Abdelgawad M.A., Abualsoud B.M., Kadi A., Ansari M.J., Deepak A. Recent Advances of Chitosan Formulations in Biomedical Applications. Int. J. Mol. Sci. 2022;23:10975. doi: 10.3390/ijms231810975.

60. Eljack S., David S., Faggad A., Chourpa I., Allard-Vannier E. Nanoparticles Design Considerations to Co-Deliver Nucleic Acids and Anti-Cancer Drugs for Chemoresistance Reversal. Int. J. Pharm. X. 2022;4:100126. doi: 10.1016/j.ijpx.2022.100126.

61. Campodoni E., Artusi C., Vazquez Iglesias B., Nicosia A., Belosi F., Vandini A., Monticelli P., Tampieri A., Sandri M. Nature-Inspired Heat and Moisture Exchanger Filters Composed of Gelatin and Chitosan for the Design of Eco-Sustainable “Artificial Noses”. ACS Appl. Polym. Mater. 2023;5:3468–3479. doi: 10.1021/acsapm.3c00140.

62. Kansız S., Elçin Y.M. Advanced Liposome and Polymersome-Based Drug Delivery Systems: Considerations for Physicochemical Properties, Targeting Strategies and Stimuli-Sensitive Approaches. Adv. Colloid. Interface Sci. 2023;317:102930. doi: 10.1016/j.cis.2023.102930.

63. Durand G.A., Amroun A., Grard G., Badaut C. Positive SARS-CoV-2 RT-QPCR of a Nasal Swab Spot after 30 Days of Conservation on Filter Paper at Room Temperature. J. Med. Virol. 2023;95:e28165. doi: 10.1002/jmv.28165.

64. Penninx B.W.J.H., Benros M.E., Klein R.S., Vinkers C.H. How COVID-19 Shaped Mental Health: From Infection to Pandemic Effects. Nat. Med. 2022;28:2027–2037. doi: 10.1038/s41591-022-02028-2.

65. Gandjour A. Cost-Effectiveness of Future Lockdown Policies against the COVID-19 Pandemic. Health Serv. Manag. Res. 2023;36:51–62. doi: 10.1177/09514848221080687.

66. Saylor D.M., Young J.A. Modeling Extraction of Medical Device Polymers for Biocompatibility Evaluation. Regul. Toxicol. Pharmacol. 2023;141:105405. doi: 10.1016/j.yrtph.2023.105405.

67. Lobo P., Vilaça J.L., Torres H., Oliveira B., Simões A. Smart Scan of Medical Device Displays to Integrate with a MHealth Application. Heliyon. 2023;9:e16297. doi: 10.1016/j.heliyon.2023.e16297.

68. Semeraro S., Gaetano A.S., Zupin L., Poloni C., Merlach E., Greco E., Licen S., Fontana F., Leo S., Miani A., et al. Operative Protocol for Testing the Efficacy of Nasal Filters in Preventing Airborne Transmission of SARS-CoV-2. Int. J. Environ. Res. Public Health. 2022;19:13790. doi: 10.3390/ijerph192113790.

69. Natu R., Herbertson L., Sena G., Strachan K., Guha S. A Systematic Analysis of Recent Technology Trends of Microfluidic Medical Devices in the United States. Micromachines. 2023;14:1293. doi: 10.3390/mi14071293.

70. Ming J., He Y., Yang Y., Hu M., Zhao X., Liu J., Xie Y., Wei Y., Chen Y. Health Technology Assessment of Medical Devices: Current Landscape, Challenges, and a Way Forward. Cost Eff. Resour. Alloc. 2022;20:54. doi: 10.1186/s12962-022-00389-6.

71. Freitas L., Vieira A.C.L., Oliveira M.D., Monteiro H., Bana e Costa C.A. Which Value Aspects Are Relevant for the Evaluation of Medical Devices? Exploring Stakeholders' Views through a Web-Delphi Process. BMC Health Serv. Res. 2023;23:593. doi: 10.1186/s12913-023-09550-0.

72. Fink M., Akra B. Comparison of the International Regulations for Medical Devices—USA versus Europe. Injury. 2023:110908. doi: 10.1016/j.injury.2023.110908.

73. Whelton P.K., Picone D.S., Padwal R., Campbell N.R.C., Drawz P., Rakotz M.K., Parati G., Zhang X.-H., Sharman J.E. Global Proliferation and Clinical Consequences of Non-Validated Automated BP Devices. J. Hum. Hypertens. 2022;37:115–119. doi: 10.1038/s41371-022-00667-z.

74. McPeck M., Moon J., Jayakumaran J., Smaldone G.C. In Vitro Model for Analysis of High-Flow Aerosol Delivery During Continuous Nebulization. Respir. Care. 2023;68:1213–1220. doi: 10.4187/respcare.10643.

75. Alanazi O., Li J. The Impact of Various HFNC Devices on Transnasal Aerosol Delivery. Respir. Care. 2023;68:10777. doi: 10.4187/respcare.10777.

76. To Quoc T., Bíró K., Pető Á., Kósa D., Sinka D., Lekli I., Kiss-Szikszai A., Budai I., Béres M., Vecsernyés M., et al. Development and Evaluation of an FDM Printed Nasal Device for CPZ Solid Nanoparticles. Molecules. 2023;28:4406. doi: 10.3390/molecules28114406.

77. Moghimipour, E.; Salimi, A.; Karami, M.; Isazadeh, S. Preparation and Characterization of Dexamethasone Microemulsion Based on Pseudoternary Phase Diagram. Jundishapur J. Nat. Pharm. Prod. 2013, 8, 105–112.

78. Boc, S.; Momin, M.A.M.; Farkas, D.R.; Longest, W.; Hindle, M. Development and Characterization of Excipient Enhanced Growth (EEG) Surfactant Powder Formulations for Treating Neonatal Respiratory Distress Syndrome. AAPS Pharm. Sci. Tech. 2021, 22, 136.

79. Srinivasan, C.; Mullen, T.J.; Hohman, J.N.; Anderson, M.E.; Dameron, A.A.; Andrews, A.M.; Dickey, E.C.; Horn, M.W.; Weiss, P.S. Scanning Electron Microscopy of Nanoscale Chemical Patterns. ACS Nano 2007, 1, 191–201.

80. Ashizawa, K. Nanosize Particle Analysis by Dynamic Light Scattering (DLS). Yakugaku Zasshi 2019, 139, 237–248.

81. Sibinovska, N.; Žakelj, S.; Kristan, K. Suitability of RPMI 2650 Cell Models for Nasal Drug Permeability Prediction. Eur. J. Pharm. Biopharm. 2019, 145, 85–95.

82. Pilicheva, B.; Draganova-Filipova, M.; Zagorchev, P.; Kassarova, M. Investigation of Betahistine Dihydrochloride Biocompatibility and Nasal Permeability In Vitro. J. Appl. Biomed. 2016, 14, 299–305.

83. Keller LA, Merkel O, Popp A. Intranasal drug delivery: opportunities and toxicologic challenges during drug development. Drug Deliv Transl Res. 2022 Apr;12(4):735-757. doi: 10.1007/s13346-020-00891-5. Epub 2021 Jan 25.

84. Cingi C, Ozdoganoglu T, Songu M. Nasal obstruction as a drug side effect. Ther Adv Respir Dis. 2011 Jun;5(3):175-82. doi: 10.1177/1753465811403348. Epub 2011 Apr 20.

85. Moffa A, Costantino A, Rinaldi V, Sabatino L, Trecca EMC, Baptista P, Campisi P, Cassano M, Casale M. Nasal Delivery Devices: A Comparative Study on Cadaver Model. Biomed Res Int. 2019 Mar 28;2019:4602651. doi: 10.1155/2019/4602651. PM

86. Patra JK, Das G, Fraceto LF, Campos EVR, Rodriguez-Torres MDP, Acosta-Torres LS, Diaz-Torres LA, Grillo R, Swamy MK, Sharma S, Habtemariam S, Shin HS. Nano based drug delivery systems: recent developments and future prospects. J Nanobiotechnology. 2018 Sep 19;16(1):71. doi: 10.1186/s12951-018-0392-8.

87. Rodríguez-Acosta GL, Hernández-Montalbán C, Vega-Razo MFS, Castillo-Rodríguez IO, Martínez-García M. Nanomedical Applications of Amphiphilic Dendrimeric Micelles. Curr Med Chem. 2021;28(38):7937-7960. doi: 10.2174/0929867328666210329125601.

88. Singh Y, Meher JG, Raval K, Khan FA, Chaurasia M, Jain NK, Chourasia MK. Nanoemulsion: Concepts, development and applications in drug delivery. J Control Release. 2017 Apr 28;252:28-49. doi: 10.1016/j.jconrel.2017.03.008. Epub 2017 Mar 6.

89. Dymek M, Sikora E. Liposomes as biocompatible and smart delivery systems - the current state. Adv Colloid Interface Sci. 2022 Nov;309:102757. doi: 10.1016/j.cis.2022.102757. Epub 2022 Aug 19.

90. Zhao C, Chen H, Wang F, Zhang X. Amphiphilic self-assembly peptides: Rational strategies to design and delivery for drugs in biomedical applications. Colloids Surf B Biointerfaces. 2021 Dec;208:112040. doi: 10.1016/j.colsurfb.2021.112040. Epub 2021 Aug 14.

91. Dib N, Silber JJ, Correa NM, Falcone RD. Amphiphilic Ionic Liquids Capable to Formulate Organized Systems in an Aqueous Solution, Designed by a Combination of Traditional Surfactants and Commercial Drugs. Pharm Res. 2022 Oct;39(10):2379-2390. doi: 10.1007/s11095-022-03342-7. Epub 2022 Jul 19.

92. Hu X, Jing X. Biodegradable amphiphilic polymer-drug conjugate micelles. Expert Opin Drug Deliv. 2009 Oct;6(10):1079-90. doi: 10.1517/17425240903158917.

93. Hu X, Jing X. Biodegradable amphiphilic polymer-drug conjugate micelles. Expert Opin Drug Deliv. 2009 Oct;6(10):1079-90. doi: 10.1517/17425240903158917.

94. Kashapov R, Gaynanova G, Gabdrakhmanov D, Kuznetsov D, Pavlov R, Petrov K, Zakharova L, Sinyashin O. Self-Assembly of Amphiphilic Compounds as a Versatile Tool for Construction of Nanoscale Drug Carriers. Int J Mol Sci. 2020 Sep 22;21(18):6961. doi: 10.3390/ijms21186961.

95. Ramazani F, Chen W, van Nostrum CF, Storm G, Kiessling F, Lammers T, Hennink WE, Kok RJ. Strategies for encapsulation of small hydrophilic and amphiphilic drugs in PLGA microspheres: State-of-the-art and challenges. Int J Pharm. 2016 Feb 29;499(1-2):358-367. doi: 10.1016/j.ijpharm.2016.01.020. Epub 2016 Jan 12.

96. Nur S, Adams CE. Chlorpromazine versus reserpine for schizophrenia. Cochrane Database Syst Rev. 2016 Apr 28;4(4):CD012122. doi: 10.1002/14651858.CD012122.pub2. PMID: 27124109;

97. Liu X, De Haan S. Chlorpromazine dose for people with schizophrenia. Cochrane Database Syst Rev. 2009 Apr 15;(2):CD007778. doi: 10.1002/14651858.CD007778. Update in: Cochrane Database Syst Rev. 2017 Apr 13;4:CD007778.

98. Quintana MC, Ramos L, González MJ, Blanco MH, Hernández L. Development of a solid phase extraction method for simultaneous determination of corticoids and tranquilizers in serum samples. J Sep Sci. 2004 Jan;27(1-2):53-8. doi: 10.1002/jssc.200301569.

99. Heng D, Lee SH, Ng WK, Tan RB. The nano spray dryer B-90. Expert Opin Drug Deliv. 2011 Jul;8(7):965-72. doi: 10.1517/17425247.2011.588206.

100. Sibinovska N, Žakelj S, Trontelj J, Kristan K. Applicability of RPMI 2650 and Calu-3 Cell Models for Evaluation of Nasal Formulations. Pharmaceutics. 2022 Feb 6;14(2):369. doi: 10.3390/pharmaceutics14020369.

101. Lea T. Caco-2 Cell Line. In: Verhoeckx K, Cotter P, López-Expósito I, Kleiveland C, Lea T, Mackie A, Requena T, Swiatecka D, Wichers H, editors. The Impact of Food Bioactives on Health: in vitro and ex vivo models [Internet]. Cham (CH): Springer; 2015. Chapter 10. DOI: 10.1007/978-3-319-16104-4

102. Kumar P, Nagarajan A, Uchil PD. Analysis of Cell Viability by the MTT Assay. Cold Spring Harb Protoc. 2018 Jun 1;2018(6). doi: 10.1101/pdb.prot095505.

103. Jespersen B, Knupp L, Northcott CA. Femoral arterial and venous catheterization for blood sampling, drug administration and conscious blood pressure and heart rate measurements. J Vis Exp. 2012 Jan 24;(59):3496. doi: 10.3791/3496.

104. Kul A, Sagirli O. A new method for the therapeutic drug monitoring of chlorpromazine in plasma by gas chromatography-mass spectrometry using dispersive liquid-liquid microextraction. Bioanalysis. 2023 Nov;15(22):1343-1354. doi: 10.4155/bio-2023-0176. Epub 2023 Oct 17.

105. Hazra A, Gogtay N. Biostatistics Series Module 3: Comparing Groups: Numerical Variables. Indian J Dermatol. 2016 May-Jun;61(3):251-60. doi: 10.4103/0019-5154.182416.

12. LIST OF PUBLICATIONS THE DISSERTATION IS BASED ON

UNIVERSITY of DEBRECEN

UNIVERSITY AND NATIONAL LIBRARY
UNIVERSITY OF DEBRECEN
H-4002 Egyetem tér 1, Debrecen
Phone: +3652/410-443, email: publikaciok@lib.unideb.hu

Registry number: DEENK/35/2025.PL
Subject: PhD Publication List

Candidate: Thinh To Quoc
Doctoral School: Doctoral School of Pharmacy

List of publications related to the dissertation

1. **To Quoc, T.**, Bíró, K., Pető, Á., Kósa, D., Haimhoffer, Á., Lekli, I., Pallér, Á., Bak, I., Gyöngyösi, A., Fehér, P., Bácskay, I., Ujhelyi, Z.: The Role of Amphiphilic Compounds in Nasal Nanoparticles.
   AAPS PharmSciTech. 25 (8), 1-14, 2024.
   DOI: http://dx.doi.org/10.1208/s12249-024-03000-8
   IF: 3.4 (2023)
2. **To Quoc, T.**, Bíró, K., Pető, Á., Kósa, D., Sinka, D. Z., Lekli, I., Kiss-Szikszai, A., Budai, I., Béres, M., Vecsernyés, M., Fehér, P., Bácskay, I., Ujhelyi, Z.: Development and Evaluation of an FDM Printed Nasal Device for CPZ Solid Nanoparticles.
   Molecules. 28 (11), 1-15, 2023.
   DOI: http://dx.doi.org/10.3390/molecules28114406
   IF: 4.2
3. **To Quoc, T.**, Bácskay, I., Fehér, P., Pallér, Á., Papp, B., Bíró, K., Ujhelyi, Z.: Personalized Nasal Protective Devices: Importance and Perspectives.
   Life (Basel). 13 (11), 1-14, 2023.
   DOI: http://dx.doi.org/10.3390/life13112116
   IF: 3.2

Total IF of journals (all publications): 10,8
Total IF of journals (publications related to the dissertation): 10,8

The Candidate's publication data submitted to the iDEa Tudóstér have been validated by DEENK on the basis of the Journal Citation Report (Impact Factor) database.

DEBRECENI EGYETEM Egyetemi és Nemzeti Könyvtár

06 February, 2025

13. KEYWORDS

nasal formulations, nanoparticles, penetration enhancers, nasal protective device

14. LIST OF ABBREVIATIONS

KEYWORD	ABBRAVIATION IN TEXT	DESCRIPTION
Active Pharmaceutical Ingredient	API	Ingredient that provides biologically active or other direct effect ingredient that provides biologically active or other direct effects
Acute Respiratory Distress Syndrome	ARDS	Symptoms include shortness of breath (dyspnea), rapid breathing (tachypnea), and bluish skin coloration (cyanosis)
Analysis of Variance	ANOVA	Statistical method that simultaneously compares means across several groups to determine if observed differences are due to chance or reflect genuine distinctions
Bovine Serum Albumin	BSA	Serum albumin protein derived from cows
Chlorpromazine	CPZ	Medication used to manage and treat schizophrenia, bipolar disorder, and acute psychosis
Chronic obstructive pulmonary disease	COPD	Inflammation, inside the airways that limit airflow into and out of the lungs
Computational Fluid Dynamics	CFD	Helps solve complex flow equations with accurate numerical methods: laminar/turbulent flow, (in)compressible fluid, multiphase flow
Dopamine receptors	D2, D3, D5	G protein-coupled receptors that are prominent in the vertebrate central nervous system (CNS)
Dulbecco′s Modified Eagle′s Medium	DMEM	High glucose culture
Evolution	E	Sub-version designation
Experimental Prototype	XP	Test fit sample
Formazan		Dyes - artificial chromogenic products obtained by reduction of tetrazolium salts

		by dehydrogenases and reductases
Fused Deposition Modeling	FDM	3D printing process that uses a continuous filament of a thermoplastic material
Gas Chromatography	GC	Common type of chromatography used in analytical chemistry for separating and analyzing compounds that can be vaporized without decomposition
Gas Chromatography – Mass Spectrometer	GC-MS	Analytical method for drug detection/ analysis
Human Colon Adenocarcinoma Caco-2 cell line	Caco-2	Transfection host
Human Nasal Epithelial cell line	RPMI 2650	form a polarized epithelium resembling nasal mucosa
2-hydroxylpropyl-β-cyclodextrin	HPBCD	Enabling excipient in pharmaceutical formulations, but also as a cholesterol modifier
International standards 10993	ISO 10993	Standards for evaluating the biocompatibility of medical devices
International standards 16890	ISO 16890	establishes an efficiency classification system of air filters for general ventilation based upon particulate matter (PM)
In Vitro Diagnostic Devices Regulation	IVDR	Requires device manufacturers to conduct clinical performance studies and provide evidence of safety and performance proportionate with a device's assigned risk class
Kolliphor EL		Nonionic surfactant used to stabilize emulsions of nonpolar materials in water
Labrafil		Water-dispersible surfactant for lipid-based formulations to solubilize and increase oral bioavailability of poorly water-soluble APIs

Labrasol		Solubilizer and skin penetration enhancer, O/W surfactant for microemulsion
Lauroglycol		Cosurfactant and solubilizer
Liquid Chromatography – Mass Spectrometer	LC-MS	Liquid chromatography separates mixtures with multiple components, mass spectrometry provides spectral information that may help to identify (or confirm the suspected identity of) each separated component
Malvern Nano Zetasizer ZSP		measure the particle size of dispersed systems from sub-nanometer to several micrometers in diameter, using the technique of Dynamic Light Scattering (DLS)
Mark	MK	Version designation
Mass Spectrometer	MS	Used to identify unknown compounds via molecular weight determination, to quantify known compounds, and to determine structure and chemical properties of molecules
Medical Devices Regulation	MDR	Comprehensive set of regulations that governs the production and distribution of medical devices in Europe
(3-(4,5-dimethylthiazol-2-yl)-2,5-diphenyltetrazolium bromide) tetrazolium Viability assay	MTT viability assay	Method for determining live cell numbers by absorbance on a microplate reader
Miglyol		Emollients
Nasal Emergency/ External Filter	NEF	Personal Protective Equipment class D/C for respiratory protection
Nasal Internal Filter	NIF	Personal Protective Equipment class D for respiratory protection
Particulate Matter	PM	contains microscopic solids or liquid droplets that are so small that they can be inhaled

		and cause serious health problems
Personal Protective Equipment	PPE	Protective clothing, helmets, goggles, or other garments or equipment designed to protect the wearer's body from injury or infection
Poloxamer		Amphiphilic structures Surfactant properties
Polymethyl methacrylate	PMMA	Synthetic polymer used as an engineering plastic
Self-Nano Emulsifying Drug Delivery System	SNEDDS	Anhydrous homogenous liquid mixtures consisting of oil, surfactant, drug and coemulsifier or solubilizer, which spontaneously form oil-in-water nanoemulsion of approximately 200 nm or less in size upon dilution with water under gentle stirring
Scanning Electron Microscope	SEM	Produces images of a sample by scanning the surface with a focused beam of electrons
SYNFASAN G3 Filter	G3	Average Arrestance (Am) of ASHRAE test dust: $80\% \leq Am < 90\%$
Thermoplastic PolyUrethane	TPU	Polyurethane plastics with many properties, including elasticity, transparency, and resistance to oil, grease, and abrasion
Transcultol		Solvent and solubilizer for solubility and bioavailability enhancement
Ultra High Performance Liquid Chromatography	UHPLC	Technique used to separate different constituents of a compound
Validating Prototype	VP	Functional sample

15. ACKNOWLEDGMENT

I would like to express my heartfelt gratitude to everyone who contributed to the completion of my PhD dissertation and supported me throughout this journey. First and foremost, I extend my deepest thanks to Professor Ildikó Katalin Bácskay, Head of the Department of Pharmaceutical Technology and Dean of the Faculty, for her invaluable guidance and encouragement. I am profoundly grateful to my supervisor, Dr. Zoltán Ujhelyi, for his unwavering support, insightful advice, and dedication throughout the entire process. I would also like to thank Professor Miklós Vecsernyés, former Dean, for his significant contributions and encouragement. Special thanks go to my coauthors, Pálma Fehér, Dóra Kósa, Ágota Pető, István Lekli, and Ádám Haimhoffer for their collaboration and invaluable input, as well as to the Department of Pharmaceutical Technology at the University of Debrecen. Without their support, this work would not have been possible. To my parents and friends, I am forever grateful for your constant encouragement, patience, and belief in me throughout this endeavor.

Finally, I give praise to the Good Lord; for the kingdom, the power, and the glory are Yours, now and forever!

16. FUNDING

Project no. TKP2021-EGA-18 has been implemented with the support provided by the Ministry of Culture and Innovation of Hungary from the National Research, Development and Innovation Fund, financed under the TKP2021-EGA funding scheme. The publication was supported by the GINOP-2.3.1-20-2020-00004, GINOP-2.3.4-15-2020-00008 and GINOP-2.3.4-15-2016-00002 projects and NKFI-143360 projects. The project was co-financed by the European Union and the European Regional Development Fund. The project was supported by project no. 2022-1.2.2-TÉT-IPARI-UZ-2022-00006 „Common research and development of different prototypes containing natural herb extract for industrial utilization".